CR 92.012

October 1992

NCEL

Contract Report

An Investigation Conducted by
Florian Mansfeld and C. H. Tsai
USC

DEVELOPMENT OF AN ELECTROCHEMICAL METHOD FOR FIELD TESTING OF PROTECTIVE COATINGS

Abstract Nine different coating systems on cold rolled steel were tested by recording EIS-data during immersion in 0.5 N NaC1 (open to air). One set of samples tested was in the as-received condition and an artificial defect applied. Another set of samples were tested after 2 year's of outdoor exposure at Cape Canaveral, FL. For this set, the susceptibility to cathodic delamination was also evaluated. The as-received condition samples were tested for 1 year. The sample with an all-latex coating was eliminated from further testing since the coating was so porous that the impedance spectra resembled those usually found for bare steel. In long term testing, alkyd/enamel, alkyd/enamel Si-alkyd, and the zinc-rich primer/epoxy polyamide/polyurethane coatings were damaged. For set of samples tested for 55 days after being outdoors, the only coating damage detected was the alkyd/enamel Si-alkyd coating. The coating properties degraded faster than the as-received sample, indicating that outdoor exposure had weakend the coating. In the cathodic delamination tests, the largest amount of damage occurred on the other alkyd-based coatings.

A theoretical analysis of the impedance of polymer coated steel was performed for the purpose of identifying parameters that could be used in the design of a coating monitor. The results of this analysis suggest that the breakpoint frequency f_b and the frequency f_{min} of the phase angle minimum F_{min} observed at the high frequencies could be used for this purpose.

NAVAL CIVIL ENGINEERING LABORATORY PORT HUENEME CALIFORNIA 93043-4328

METRIC CONVERSION FACTORS

Approximate Conversions to Metric Measures

Symbol	When You Know	Multiply by	To Find	Symbol
		LENGTH		
in	inches	*2.5	centimeters	cm
ft	feet	30	centimeters	cm
yd	yards	0.9	meters	m
mi	miles	1.6	kilometers	km
		AREA		
in^2	square inches	6.5	square centimeters	cm^2
ft^2	square feet	0.09	square meters	m^2
yd^2	square yards	0.8	square meters	m^2
mi^2	square miles	2.6	square kilometers	km^2
	acres	0.4	hectares	ha
		MASS (weight)		
oz	ounces	28	grams	g
lb	pounds	0.45	kilograms	kg
	short tons (2,000 lb)	0.9	tonnes	t
		VOLUME		
tsp	teaspoons	5	milliliters	ml
Tbsp	tablespoons	15	milliliters	ml
fl oz	fluid ounces	30	milliliters	ml
c	cups	0.24	liters	l
pt	pints	0.47	liters	l
qt	quarts	0.95	liters	l
gal	gallons	3.8	liters	l
ft^3	cubic feet	0.03	cubic meters	m^3
yd^3	cubic yards	0.76	cubic meters	m^3
		TEMPERATURE (exact)		
°F	Fahrenheit temperature	5/9 (after subtracting 32)	Celsius temperature	°C

*1 in = 2.54 (exactly). For other exact conversions and more detailed tables, see NBS Misc. Publ. 286, *Units of Weights and Measures*, Price $2.25, SD Catalog No. C13.10:286.

Approximate Conversions from Metric Measures

Symbol	When You Know	Multiply by	To Find	Symbol
		LENGTH		
mm	millimeters	0.04	inches	in
cm	centimeters	0.4	inches	in
m	meters	3.3	feet	ft
m	meters	1.1	yards	yd
km	kilometers	0.6	miles	mi
		AREA		
cm^2	square centimeters	0.16	square inches	in^2
m^2	square meters	1.2	square yards	yd^2
km^2	square kilometers	0.4	square miles	mi^2
ha	hectares (10,000 m^2)	2.5	acres	
		MASS (weight)		
g	grams	0.035	ounces	oz
kg	kilograms	2.2	pounds	lb
t	tonnes (1,000 kg)	1.1	short tons	
		VOLUME		
ml	milliliters	0.03	fluid ounces	fl oz
l	liters	2.1	pints	pt
l	liters	1.06	quarts	qt
l	liters	0.26	gallons	gal
m^3	cubic meters	35	cubic feet	ft^3
m^3	cubic meters	1.3	cubic yards	yd^3
		TEMPERATURE (exact)		
°C	Celsius temperature	9/5 (then add 32)	Fahrenheit temperature	°F

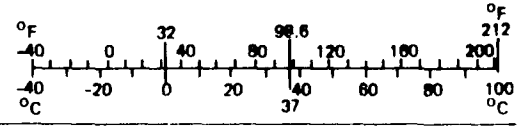

REPORT DOCUMENTATION PAGE

Form Approved
OMB No. 0704-018

1. AGENCY USE ONLY (Leave blank)	2. REPORT DATE	3. REPORT TYPE AND DATES COVERED
	October 1992	Final; 1 July 1990 - 31 December 1991

4. TITLE AND SUBTITLE DEVELOPMENT OF AN ELECTRO-CHEMICAL METHOD FOR FIELD TESTING OF PROTECTIVE COATINGS

5. FUNDING NUMBERS

C - N00014-90-J-4123

6. AUTHOR(S)

Florian Mansfeld and C. H. Tsai

7. PERFORMING ORGANIZATION NAME(S) AND ADDRESS(ES)

University of Southern California
Materials Science & Engineering
University Park, VHE 602
Los Angeles, CA 90089-0241

8. PERFORMING ORGANIZATION REPORT NUMBER

CR 92.012

9. SPONSORING/MONITORING AGENCY NAME(S) AND ADDRESS(ES)

Chief of Naval Research / Naval Civil Engineering Laboratory
Office of Naval Technology Materials Science Div., Code L52
800 No. Quincy Street Port Hueneme, CA 93043-4328
Arlington, VA 22217-5000

10. SPONSORING/MONITORING AGENCY REPORT NUMBER

11. SUPPLEMENTARY NOTES

12a. DISTRIBUTION/AVAILABILITY STATEMENT

Approved for public release; distribution is unlimited.

12b. DISTRIBUTION CODE

13. ABSTRACT *(Maximum 200 words)*

Nine different coating systems on cold rolled steel were tested by recording EIS-data during immersion in 0.5 N NaCl (open to air). One set of samples tested was in the as-received condition and an artificial defect applied. Another set of samples were tested after 2 year's of outdoor exposure at Cape Canaveral, FL. For this set, the susceptibility to cathodic delamination was also evaluated. The as-received condition samples were tested for 1 year. The sample with an all-latex coating was eliminated from further testing since the coating was so porous that the impedance spectra resembled those usually found for bare steel. In long term testing, alkyd/enamel, alkyd/enamel Si-alkyd, and the zinc-rich primer/epoxy polyamide/polyurethane coatings were damaged. For set of samples tested for 55 days after being outdoors, the only coating damage detected was the alkyd/enamel Si-alkyd coating. The coating properties degraded faster than the as-received sample, indicating that outdoor exposure had weakend the coating. In the cathodic delamination tests, the largest amount of damage occurred on the other alkyd-based coatings.

A theoretical analysis of the impedance of polymer coated steel was performed for the purpose of identifying parameters that could be used in the design of a coating monitor. The results of this analysis suggest that the breakpoint frequency f_b and the frequency f_{min} of the phase angle minimum F_{min} observed at the high frequencies could be used for this purpose.

14. SUBJECT TERMS

Polymer coatings, impedance spectroscopy, corrosion, delamination, monitoring, degradation, steel, exposure test, coating damage

15. NUMBER OF PAGES

50

16. PRICE CODE

17. SECURITY CLASSIFICATION OF REPORT	18. SECURITY CLASSIFICATION OF THIS PAGE	19. SECURITY CLASSIFICATION OF ABSTRACT	20. LIMITATION OF ABSTRACT
Unclassified	Unclassified	Unclassified	UL

Table of Contents

Development of an Electrochemical Method for Field Testing of Protective Polymer Coatings

F. Mansfeld and C. H. Tsai
Corrosion and Environmental Effects Laboratory (CEEL)
Department of Materials Science & Engineering
University of Southern California
Los Angeles, CA 90089-0241

1.0 Introduction

The application of polymer coatings is one of the most common methods of corrosion protection. In fact, steel structures are rarely exposed without corrosion protection by a coating system. In considering the cost of corrosion protection by polymer coatings, one has to take into account the cost for labor of coating application which amounts to several times the cost of the paint. Considering these data and the fact that the Navy uses extremely large amount of paint for its fleet and other installations, it becomes obvious that a method, which would give an indication when a paint systems has to be replaced, would be very useful. Such an approach could be considered a "retirement for cause" approach replacing a paint cycle which is based solely on the time the system has been in service.

Electrochemical impedance spectroscopy (EIS) has been shown to be a very powerful technique for the study of the properties of coatings including the corrosion resistance of polymer coated metals (1-3). With EIS changes of the properties of a coating system during exposure to a corrosive environment such as the ocean leading to delamination and corrosion at the coating/metal interface can all be determined from the analysis of the impedance spectrum. The success demonstrated with EIS in laboratory studies suggests that EIS could also form the basis instrumentation for field testing of Navy coating systems. While the design of such instrumentation would be based on the EIS-technique, one would not want to collect the entire impedance spectrum, but measure certain characteristic parameters preferably in the high-frequency range to shorten the measurement time.

In this project, a theoretical analysis of the impedance behavior of polymer coated steel has been carried out with the aim of determining those parameters which are related to coating degradation and corrosion at the coating/metal interface. The concepts developed in this study have

then been tested using coating systems prepared at the Naval Civil Engineering Laboratory in Port Hueneme, California. The same coating systems were tested in the as-received condition and after two years outdoor exposure in Florida.

2.0 Theoretical Studies

Theoretical studies of the changes of the impedance spectra of a polymer coated metal exposed to a corrosive environment have been performed using the model shown in Fig. 1, where C_c is the coating capacitance, R_{po} the coating resistance ("pore resistance"), C_{dl} the capacitance at the area under the coating where corrosion occurs and R_p is the corresponding polarization resistance (1-3). R_Ω is related to the electrolyte resistance and the ohmic resistance in electrical leads, etc.

When a coating on metal is still protective, the impedance spectrum shows only one time constant with a wide linear capacitive region at which the slope equals minus one and the phase angles close to 90 degrees. As the coating degrades due to the penetration of electrolyte into the coating and the occurrence of corrosion under the coating, the impedance spectrum change from one time constant to two time constants. The first time constant at higher frequencies is associated with the properties of the coating while the second one at lower frequencies is related to the degree of corrosion. Since ionic current through the degraded coating is concentrated at the corroded area (delaminated area), the magnitudes of R_{po}, C_{dl}, and R_p should be related to this area. However, it is difficult to build an instrument for field testing of protective coatings based on these equivalent-circuit parameters because it requires a complicated and very time-consuming process of data analysis.

Recently, modelling of EIS-data for coating delamination has been introduced by Haruyama et al (4). They have suggested that the decrease of R_{po} and R_p and the increase of C_{dl} with exposure time is due to an increase of the delaminated area A_d according to:

$$R_{po} = R^o_{po}/A_d \qquad (1)$$

$$R_p = R^o_p/A_d \qquad (2)$$

$$C_{dl} = C^o_{dl}A_d \qquad (3)$$

where $R^o_{po} = \rho \cdot d$ (ohm.cm^2) (4)

R^o_p (ohm.cm^2) and C^o_{dl} (μF/cm^2) are characteristic values for the corrosion reaction at the coating/metal interface and ρ is the coating resistivity.

The coating capacitance C_c (μF) depends on the total sample area A, the thickness of the coating d and its dielectric constant ε :

$$C_c = (\varepsilon\varepsilon_o/d)A = C^o_c A, \quad (5)$$

Haruyama et al have (4) have suggested that the extent of delamination can be determined experimentally from the breakpoint frequency f_b, which is the impedance at the phase angle $\Phi = 45^o$:

$$f_b = 1/2\pi R_{po}C_c = (1/2\pi R^o_{po}C^o_c)(A_d/A)$$
$$= (2\pi\varepsilon\varepsilon_o\rho)^{-1}(A_d/A) = f^o_b D \quad (6)$$

where

$D = A_d/A = f_b/f^o_b$

is the delamination ratio and

$$f^o_b = 1/2\pi\varepsilon\varepsilon_o\rho \quad (7)$$

is a characteristic parameter which depends only on the coating parameters ε and ρ and is independent of coating thickness. In Haruyama's approach (4) it is assumed that coating properties such as the resistivity ρ and dielectric constant ε do not change with exposure time. The results obtained in this study for coating systems used by the U.S. Navy show that this assumption is oversimplified.

In addition to the breakpoint frequency f_b , Mansfeld et al have suggested (5,6) that the minimum of the phase angle Φ_{min} and its frequency f_{min} can also be used to characterize the extent of delamination. Using the equivalent circuit in Fig. 1 and certain simplifying assumptions, they have shown that the following relationships apply:

$$f_{min} = (1/4\pi^2 C_c C_{dl} R^2_{po})^{1/2} = (D/4\pi^2 \varepsilon\varepsilon_o C^o_{dl} \rho^2 d)^{1/2} = a''_2 (D/d)^{1/2} \quad (8)$$

$$\tan \Phi_{min} = (4C_c/C_{dl})^{1/2} = (4\varepsilon\varepsilon_o/C^o_{dl} dD)^{1/2} = a''_3 (dD)^{-1/2}, \quad (9)$$

$$\log f_b = a_1 + b_1 \log D = a_1 + \log D, \quad (10)$$

$$\log f_{min} = a_2 + b_2 \log D = 1/2 \log a_2'/d + 1/2 \log D, \quad (11)$$

$$\log \Phi_{min} = a_3 + b_3 \log D = 1/2 \log a_3'/d - 1/2 \log D, \quad (12)$$

$$f_b/f_{min} = (C_{dl}/C_c)^{1/2} = (dC^o_{dl} D/\varepsilon\varepsilon_o)^{1/2} = a_4 D^{1/2} \quad (13)$$

$$\log (f_b/f_{min}) = \log a_4' + 1/2 \log D \quad (14)$$

Mansfeld et al (5,7) have argued that in considering the use of the breakpoint frequency f_b for the determination of the delaminated or corroded area A_d one has to consider that both ε and ρ are expected to change with exposure time. Due to water uptake of the coating ε will increase, while ρ will decrease as conductive paths and defects develop in the coating. In Eq. 7, f^o_b is therefore not a constant value, but is likely to change with exposure time as ε increases and ρ decreases. In order to decide whether an observed increase of f_b is due to changes in D or ρ, Mansfeld et al (7) have proposed the use of the ratio f_b/f_{min} (Eq.13,14), which is independent of the coating resistivity ρ. Since Φ_{min} is also independent of ρ (Eq. 9), this parameter can be used for the same purpose. This approach will be used in this study for the analysis of the corrosion behavior of steel coated with various paint systems used by the U.S. Navy.

Fig. 2 shows theoretical impedance spectra for three coating thicknesses d ranging from 10 μm (Fig. 2a) to 1000 μm (Fig. 2c) and for different delamination ratios D (1). It can be seen that very little delamination causes large changes in the spectra and the appearance of two time constants for thin coatings. However, for thicker coatings (Fig. 2c) it is difficult to detect the second time constant at the lowest frequencies. With increasing coating delamination (D increases), f_b and f_{min} move to higher frequencies , while Φ_{min} becomes smaller.

Fig.3 shows the dependence of f_b, f_{min} and Φ_{min} on D according to Eq. 10-12 for three coating thicknesses. Since both f_b and f_{min} are determined in the high-frequency range the measurement time for these parameters is

very short. It should be noted that f_{min} and Φ_{min} are determined in the same measurement. An instrument which measures coating damage based on one of these three parameters would determine impedance data starting between 10 and 100 kHz, scan to lower frequencies and stop the measurement when the parameter of interest has been detected.

Another possibility to determine coating damage uses the measurement of the impedance at two frequencies. If these frequencies are located in the capacitive region, where the slope of the log /Z/ - log f curve has a value of -1, then the ratio of the two measured impedance data is the same as the ratio of the frequencies. With increasing coating damage, this ratio R decreases. In Fig. 4 the ratios R_1 and R_2 are plotted as a function of D, where R_1 and R_2 are defined as:

$$R_1 = \log (Z_{100}/Z_{10000}) \qquad (15a)$$

$$R_2 = \log (Z_1/Z_{100}), \qquad (15b)$$

with Z_i being the impedance for the frequency f_i. For a perfect coating, for which the impedance is capacitive in the entire frequency region, $R_1=R_2=1$. If a contribution from R_{po} appears in the frequency range in which R_1 or R_2 are determined, R_1 and/or R_2 will decrease with decreasing R_{po}. R_1, which is determined at the higher frequencies, is independent of the coating thickness d and is most sensitive to coating damage for values of D between 0.1 and 10%. R_2 depends slightly on d for thin coatings and is most useful for D-values smaller than 0.1%. R_2 is therefore more applicable in the very early stages of coating degradation.

3.0. Experimental Approach

3.1 Polymer Coatings

Table 1 shows the coating systems on cold rolled steel tested in this study. All coating systems were prepared at the Navy Civil Engineering Laboratory (NCEL), Port Hueneme, CA according to Steel Structures Painting Council Paint Specifications and Navy coating application standards. In most systems a primer is covered by two layers of a topcoat. These coatings are numbered CR#1-9 in this report. For CR#1 and 2 a Zn-chromate alkyd primer was used, for CR#3 and 4 a zinc oxide-iron oxide alkyd primer was used, coatings #5 and 6 had a organic zinc-rich primer, CR#7 and 9 were covered with an epoxy polyamide primer

and in CR#8 a latex primer was used. The second and third coating layers consisted of enamel alkyd and enamel silicon alkyd for CR#1-4 and of epoxy polyamide or polyurethane for CR#5-9.

In the first part of this investigation, the as-received samples CR#1, 2, 5, 6, 8, and 9 were tested. For CR#8, which consists of a latex primer and a latex topcoat, it was found that the coating was apparently so porous that the impedance spectra resembled those of bare steel even after only 2 h exposure to 0.5 N NaCl . This coating system was therefore not tested any further. In the second part of this study CR#1, 2, 3 ,4, 5, 7, and 9 were tested after two years outdoor exposure at Cape Canaveral, Florida during 3/89 and 3/91.

3.2 Experimental Procedure for Impedance Measurements

The coated steel samples were exposed in the electrochemical cell shown in Fig. 5. The exposed coating area was 20 cm^2. A round stainless steel plate (15 cm^2) and a saturated calomel electrode (SCE) served as counter (CE) and reference electrode (REF), respectively. A platinum wire was coupled through a 2 μF capacitor with the reference electrode in order to eliminate phase shift which occurs in the highest frequencies range due to phase shift from the reference electrode (8).

The EIS-data were obtained using a Solartron 1286 potentiostat and a Solartron 1250 frequency response analyzer (FRA), which were controlled by an American XT computer (Fig. 6). In order to optimize the quality of the EIS-data, various current measuring resistors of the potentiostat, integration times (and/or cycles) and ac signal amplitudes were applied to the system in a frequency range between 65 kHz and 10 mHz depending on the impedance of the system. The rule of thumb is to maintain a high signal-to-noise ratio, but avoid current overload. In the high frequency range (above 1 Hz), the impedance of the coating system was usually not too high so that a lower signal amplitude (10-20 mV) and integration time (10 seconds with auto integration off) were used. The initial current measuring resistor was set to within one order less than the impedance at 65 kHz to avoid current overload. Using software developed at CEEL it was increased automatically as the measured impedance increased with decreasing frequency. In the lower frequency range (below 1 Hz), a higher amplitude ac signal (30-100 mV) and longer integration times (10 cycles with auto integration on) were used. For the potentiostat, the low pass filter was turned on at frequencies below 10 Hz and the measuring resistor was set as before until the maximum value of

10^5 ohm was reached. For samples with an artificial defect, for which the ionic current through the hole was usually high enough to provide a good signal-to-noise ratio, an ac signal of 5-10 mV amplitude was applied in the whole frequency range.

3.3 Experimental Procedure for Different Coating Systems

In the first part of this project, an as-received sample and a sample containing a drilled pore of 0.07 cm diameter were exposed to 0.5 N NaCl solution for the coating systems CR#1, 2, 5, 6, 8 and 9. The EIS-data were determined at E_{corr} for both types of samples as a function of exposure time. In the second part of this study, EIS-data were determined for coating systems which had been exposed outdoors at the NCEL Marine Atmospheric Test Site in Cape Canaveral, Florida for more than two years (CR#1, 2, 3, 4, 5, 6, 7, and 9). An as-received sample for each coating system was exposed to 0.5 N NaCl solution. For another sample which contained an artificial defect of 0.05 cm diameter, cathodic disbonding experiments were carried out for a 24 h period.

The impedance measurements were performed under potentiostatic control at the open-circuit potential or corrosion potential E_{corr}. If there was no stable E_{corr} for very protective coating systems such as CR#6 and CR#9, a potential which is equal to E_{corr} for bare steel exposed to the same corrosive environment was applied to the system, i.e. -600 mV vs SCE. In the initial stages of exposure, EIS-data were measured at first after two hours, one day, two days, four days and one week exposure. After that, a more flexible schedule was followed. The more the spectra changed, the more frequently EIS-data were determined (about three times a week). The data were analyzed with the COATFIT software program developed at CEEL, which is based on the model in Fig.1. In addition parameters such as f_b, f_{min}, Φ_{min}, R_1 and R_2 were determined for each exposure time (Eq. 6-15).

The cathodic disbonding experiments were performed for coatings which had been exposed outdoors. In these experiments, a sample containing an artificial defect was held at a constant cathodic potential E = -1250 mV vs SCE and the polarization current was recorded. Cathodic polarization was interrupted after 1h, 6h and 24h for impedance measurements, which were started after a stable E_{corr} was established (usually within about 15 min.). Scotch tape was applied to the area around the hole after 24 hours cathodic polarization and then pulled away in order to determine the actual delaminated area A_d.

4.0 Experimental Results

4.1. Samples without Outdoors Exposure

As-received samples were exposed to 0.5 N NaCl at E_{corr} for about one year. Since for most samples very little degradation occurred during this time, samples containing an artificial defect were also exposed in order to determine the extent of coating delamination originating from this defect.

4.1.1. As-Received Samples

Visual observation of the samples under a microscope after one year exposure to 0.5 N NaCl showed blistering and rust spots for CR#1, 2 and 5 and only very few rust spots of less than 0.1 mm diameter for CR#6 and 9. For CR#1 several rust spots and about 15 blisters were observed on the 20 cm^2 exposed surface. The rust spots and blisters covered about 1% of the total surface area. For CR#2 a large broken blister of about 8 mm diameter which was covered with rust was the major coating damage. In addition a very large number of small blisters of about 1 mm diameter was found on the entire coating surface. For CR#5 several small rust spots, but no blisters were detected.

Fig. 7 shows the impedance spectra for CR#2 (Zn-chromate alkyd, enamel silicon alkyd) after 43, 90 and 162 days exposure to 0.5 N NaCl. The impedance spectra changed from the capacitive nature typical for an intact coating to spectra exhibiting two time constants with increasing exposure time. At intermediate frequencies the spectra are dominated by the pore resistance R_{po}. The breakpoint frequency f_b and the frequency f_{min} of the minimum phase angle Φ_{min} shift to higher frequencies, while Φ_{min} decreases. These changes indicate that the coating deteriorates as moisture penetrates the coating, defects occur in the coating and corrosion starts at the coating/metal interface. For CR#6 it was found that different impedance spectra could be obtained for the two sides of the panel. One side would give EIS-data usually found for very protective coatings, while for the other side the spectra were similar to those typically found for damaged or very porous coatings. This finding points to a quality control problem for this coating system (zinc-rich primer/epoxy polyamide/latex) which can be detected in a very short time with EIS. It was also found that removal of the topcoat did not change the impedance spectra significantly. The remaining tests for CR#6 were carried out with a sample which initially had a very high impedance.

The results of the analysis of the EIS-data for coating systems CR#1, 2, 5, 6 and 9 are shown in Fig. 8 a-d. The coating capacitance C_c is the lowest for CR#9, which apparently has the thickest coating layer (Fig. 8a). Coatings CR#1, 2 and 5 seem to have the same thickness. The initial increase of C_c is related to water uptake by the coating. Degradation of the coating was indicated for CR#1, 2, and 5. Fig. 8b shows that the pore resistance R_{po} decreases the most for coating CR#2. After about one year exposure R_{po} is the lowest for CR#2, which is the enamel alkyd system, followed by CR#1 and #5. A continuous increase of the double layer capacitance C_{dl} (Fig. 8c) can be considered as evidence that the area at which delamination and/or corrosion occur is increasing (Eq.3). This increase occurs first and is the largest for CR#2 and 5, which indicates that these coating systems provide the least corrosion protection. The decrease of R_p, which suggests an increase of the corrosion rate at the metal/coating interface at constant A_d , is the largest for CR#2 followed by CR#1 and 5 (Fig. 8d). This analysis of EIS-data for the five coating systems shows qualitatively that the coatings CR#1, 2 and 5 suffer degradation during exposure to NaCl for one year, while the coatings CR#6 and 9 remain more or less unchanged.

The breakpoint frequency f_b increased the most for coating CR#2 and to a lesser extent for CR#1 and 5 (Fig. 9a). These three coatings have apparently deteriorated more than CR#6 and 9. The values of the minimum phase angle Φ_{min} and its frequency f_{min} could be detected only for CR#1, 2 and 5 (Fig. 9b and 9c). After about one year f_{min} has increased to the highest frequency for CR#2 and has the lowest value for CR#1. However, Φ_{min} has the same value for CR#1 and 2 and a higher value for CR#5. As discussed above, Φ_{min} depends only on the coating resistivity ρ, while f_{min} depends on both D and ρ (Eq. 6-9).

Fig. 10 a-e shows the time dependence of R_1 and R_2 for the five coating systems. Only coatings CR#1, 2 and 5 showed a significant decrease of R_1 and R_2 from the value of 2 for an undamaged coating. One can estimate based on the calibration curves for R_2 (Fig. 4) that D was about 0.04% for CR#1 after 160 days exposure. For CR#2 the value of R_1 at the same time leads to D = 3%. The data for CR#5 are more difficult to analyze, however D = 6% seems to be a reasonable value.

4.1.2. Samples with an Artificial Defect

Since not much coating damage had occurred after about six months exposure to 0.5 N NaCl for the as-received coatings, a new test series was

started in which a small hole of 0.07 cm diameter were drilled through the coating into the steel. This approach allowed to determine the collection of impedance data for samples with significant coating damage and the comparison of propagation rates of coating delamination originating from these artificial pits for the different coating systems as a function of exposure time.

Fig. 11 a-d show the impedance spectra after 24h and 44d immersion in NaCl. The spectra are dominated by the resistance R_h of the solution in the defect in the artificial defect and the R_p- and C_{dl}-values in the defect (Fig. 1). After 24 h the impedance spectra were fairly similar for the five coating systems (Fig. 11a and b). However, after 44 d there was a clear difference in the spectra for CR#1, 2 and 5 and for CR#6 and 9 (Fig. 11c and d). R_h for CR#9 increased markedly with time most likely as a result of the plugging of the artificial defect with corrosion products.

The time dependence of E_{corr} is shown in Fig. 12 and the results of the analysis of the EIS-data are displayed in Fig. 13. E_{corr} for CR#5 and 6, which contain an organic zinc-rich primer, was very negative initially, but then exhibited a different time dependence with only CR#9 maintaining the very negative potential typical of zinc (Fig. 12). The time dependence of R_h is given in Fig. 13 a. As mentioned before, the increase of R_h for CR#9 is different from the more less constant value for the other coatings. The pronounced increase of C_{dl} for CR#5 in Fig. 13b is related to the increase of the delaminated and/or corroding area A_d and therefore to D. It is surprising that C_{dl} had the lowest value for CR#5 for which the data obtained for the as-received samples indicated rather poor performance. The decrease of R_p in Fig. 13c was the most pronounced for CR#1 and 2 which is similar to results for the undamaged coatings (Fig. 8d). For CR#5, 6 and 9 R_p did not show any significant changes with exposure time. Since the impedance is dominated by the reactions in the defect, f_{min} (Fig. 14a) and Φ_{min} (Fig. 14b) are independent of exposure time.

Visual observation of the samples containing an artificial defect after exposure for 45 days showed that rust was flowing down from the defect for CR#1 and 2, but not for CR#5 and 6. The latter two coating systems apparently provided cathodic protection through the zinc in the primer. For CR#9 a very compact rust layer was covering the defect.

4.2. Samples Tested After Outdoors Exposure

Samples which had been exposed in Florida for two years were tested by recording of EIS-data during immersion in 0.5 N NaCl for 55d. In addition,

cathodic delamination tests were performed in order to determine the relative resistance to coating delamination for the different coating systems.

4.2.1 Samples without an Artificial Defect

The samples which had been exposed outdoors for two years were all rated 10 according to ASTM Standard D 610-85. After 55 days exposure to 0.5 N NaCl CR#2 degraded to a rating of 5 with more than 3% of the total area covered by rust spots. The other coating systems remained intact. This result is confirmed by the impedance spectra shown in Fig. 15 a-d which show the occurrence of two time constants for CR#2 after 30 days exposure, while the impedance for the other coating systems remain capacitive. The results of the analysis of impedance data for CR#1, 2, 3, 4, 5, 6, 7 and 9 are shown in Fig 16 a-c. The coating capacitance C_c is the lowest for CR#9 (Fig. 16a). The effect of water uptake was more pronounced for CR#2 than for the other coatings which implies that outdoor exposure has increased the deterioration of this coating system. This can also be seen from the fact that R_p for CR#2 (Fig. 16b) decreased to 8000 ohms after only 55 days exposure to NaCl, while for the same coating system without outdoor exposure R_p was $2x10^7$ ohms for the same exposure time (Fig. 8d). The breakpoint frequency f_b increased to 4000 Hz after 55 days (Fig. 16c), while in Fig. 9 a f_b was only 10 Hz.

Fig. 17 a-h show the time dependence of R_1 and R_2 for the eight coating systems after atmospheric exposure. Only CR#2 showed a significant decrease of R_1 and R_2 from the value of 2 for an undamaged coating. For CR#2 one can estimate based on the calibration curves in Fig. 4 that D was about 4% after 55 days exposure. This agrees with visual observation which showed 3.2% rusted area according to ASTM D610-85.

Fig. 18 a-d gives a comparison of the time dependence of f_b, f_{min}, $\tan\Phi_{min}$ and f_b/f_{min} for as-received CR#2 and CR#2 which had been exposed outdoors in Florida for two years. Both f_b and f_{min} increased to the same levels in about half the time for the samples which had been exposed outdoors. Φ_{min} dropped in 55 d to the values observed for the as-received samples in 100 d. These results suggest that after outdoor exposure CR#2 deteriorates faster during immersion in NaCl due to the damage to the coating produced by pollutants and UV light .

4.2.2 Cathodic Delamination

Cathodic delamination experiments were carried out at E = -1250 mV vs SCE, where water reduction occurs resulting in copious amounts of OH^- which can cause coating delamination. Fig. 19 shows the impedance spectra for CR#1 after cathodic polarization for 1h, 6h and 24h. Very large changes in the impedance spectra were observed after 6 h with the spectra changing from those for the intact coating being observed after 1 h at the higher frequencies to spectra typical of coatings containing an artificial defect (Fig. 11). The drastic changes in the spectra after 6 h and 24 h polarization suggest that cathodic delamination has propagated from the artificial defect with increasing polarization time. The capacitive region in the low and intermediate frequency range is considered to be due to the double layer capacitance C_{dl} in the original defect and the growing delaminated area.

Fig. 20 shows the cathodic currents for the three times at which EIS-data were recorded. The current increased markedly for coatings with severe delamination, i.e. CR#1, #2, #3, and #4 and levelled off at about 10 μA for coatings with less delamination, i.e. CR#5, #6, #7, and #9. The increase of the polarization current is attributed to the increased delaminated area. This conclusion agrees with the results of visual examination after the tape test which indicate that CR#1, 2, 3, and 4 had 2.2%, 2.5%, 15.0%, and 2.0% delamination, respectively, after 24 h cathodic polarization, while CR#5, 6, 7, and 9 did not show noticeable delamination.

In Fig. 21 the results of the analysis of the impedance spectra for the coating systems with cathodic polarization at E = -1250 mV are summarized. For coatings CR#1, 2, 3, and 4, which showed significant delamination after 24 hours cathodic polarization, the double layer capacitance C_{dl} increased markedly with the exposure time, while for CR#5, 6, 7 and 9, for which delamination was not observed, C_{dl} remained more or less constant. The resistance R_h related to the ohmic resistance in the defect and in the delaminated area showed similar changes as C_{dl} for the two groups of coating systems, which can be expected since both parameters are related to the active electrode surface area A_d.

The results of the visual analysis of the degree of delamination after the tape test can be compared with the impedance data using Eq. (1) and (3) based on the values of R_h = 10 ohm.cm^2 and C^o_{dl} = 1270 μF/cm^2 which were the average values for those samples for which delamination was not observed after 1 h. A_d was also calculated assuming that the cathodic current density remains constant throughout polarization and increasing delamination. This means that the measured current will increase with increasing A_d. Fig. 22 shows a comparison of the calculated delaminated

area A_d based on R_h, C_{dl} and the cathodic current with A_d as determined by visual observation after the tape pull test for CR#1, 2, 3, and 4 which showed significant coating delamination after 24 hours cathodic polarization. There is good correlation between these values except for A_d based on the measured current for CR#3.

5.0 Discussion

The discussion of the results obtained in this project will consist of two parts. In the first part the performance of the different coating systems on cold rolled steel as determined with EIS will be discussed. In the second part the use of different parameters which can obtained with impedance measurements in a commercial instrument for the determination of coating properties in field applications will be illustrated.

5.1 Performance of Coating Systems

In the first part of this project the performance of the coating systems CR#1, 2, 5, 6, 8 and 9 on cold rolled steel (Table 1) was studied by immersion in 0.5 N NaCl and recording of impedance spectra. The samples were exposed as-received and after drilling of a small hole. In the evaluation of the as-received samples coating system CR#2, which was an all Latex system, was eliminated from further study when it was found that the coating was so porous that the EIS-data were similar to those for bare steel after only 2 hours immersion in NaCl. The impedance spectra remained capacitive for one year for CR#6 (zinc-rich primer/epoxy polyamide/latex) and CR#9 (epoxy polyamide). This behavior indicates that no conductive paths between the coating and the metal had developed. Therefore the impedance spectra are those for the intact coating. For CR#1, 2 and 5 changes in the spectra were observed with the EIS-data being in agreement with the EC in Fig. 1. These data can therefore be analyzed with the software COATFIT. As shown in Fig. 8 b the pore resistance R_{po} could be detected already after very short exposure times. R_{po} first decreased for CR#2 (alkyd/enamel Si-alkyd). For CR#1 (alkyd/enamel alkyd) a sudden increase occurred after about 40 d followed by a gradual decrease after about 200 d. CR#5 (zinc-rich primer/epoxy polyamide/polyurethane) showed small changes with exposure time around an average value. The time dependence of R_{po} shown in Fig. 8 b is different from that observed by Mansfeld et al (1-3) for a polybutadiene coating on steel, where a continuous decrease of R_{po} was observed. The electrode capacitance C_{dl} increased continuously for

CR#2 from about 10^{-8} F to about 10^{-4} F, while for CR#5 an increase of C_{dl} was observed after about 225 d (Fig. 8c). For CR#1 C_{dl} only showed small fluctuations around an average value. The polarization resistance R_p, which similar to C_{dl} is also proportional to the active metal area at which corrosion and delamination occur (Fig. 8d). For CR#2 the largest decrease is observed followed by CR#1 and 5.

As discussed above (2.0) certain parameters, which are related to coating deterioration, can be determined directly from the spectra without any analysis. Fig. 9 shows the time dependence of f_b, f_{min}, Φ_{min} and f_b/f_{min}. The breakpoint frequency f_b (Fig. 9a) shows the same time dependence as R_{po} (Fig. 8b) with f_b increasing by a factor of about 10^4 for CR#2 and showing smaller increases for CR#1 and 5. Values for f_{min} and Φ_{min} could only detected for CR#1, 2 and 5 (Fig. 9b and c). For CR#2 f_{min} was observed after about 100 d, for CR#1 f_{min} and Φ_{min} were first detected after 245 d and for CR#5 these parameters could first be recorded after 220 d. An important result concerning the mechanism of coating degradation can be obtained by a comparison of the numerical values and changes with time of f_{min} (Fig. 9b) and Φ_{min} (Fig. 9c). For f_{min} a constant increase with time was observed for CR#2, while for CR#1 and 5 f_{min} was more or less constant, but different by about a factor of 10 (Fig. 9b). Φ_{min} has the same values for CR#1 and 2, but is higher for CR#5. Similarly, the ratio f_b/f_{min} seems to be independent of time for CR#1 and 5, but increases for CR#2. The lowest f_b/f_{min} ratio was observed for CR#5 for which the lowest degree of delamination was indicated by visual examination.

At this time it is necessary to expand the analysis given in Section 2.0 in which only the dependence of the parameters which can be obtained from EIS-data on coating thickness d, delaminated area A_d and delamination ratio D was considered. As already mentioned above changes due to the decrease of the coating resistance ρ have also be taken into account in the analysis of the degradation of polymer coatings. This leads to the following relationships in which the dependence on ρ, A_d and D is considered:

$$R_{po} = \rho\, d/ A_d = \rho\, d/D\, A \qquad (16)$$

$$f_b = K^o_b\, D/\rho \qquad (17a)$$

$$K^o_b = (2\pi\varepsilon\varepsilon_o)^{-1} \qquad (17b)$$

$$f_{min} = a_2''' (D)^{1/2} \rho^{-1} \quad (18a)$$

$$a_2''' = (2\pi)^{-1} (\varepsilon\varepsilon_o C^o_{dl} d)^{-1/2} \quad (18b)$$

$$= (2\pi d)^{-1} (C^o_c C^o_{dl})^{-1/2} \quad (18c)$$

$$\tan \Phi_{min} = a_3''' (D)^{-1/2} \quad (19a)$$

$$a_3''' = 2 (\varepsilon\varepsilon_o)^{1/2} (C^o_{dl} d)^{-1/2} \quad (19b)$$

$$= 2 (C^o_c / C^o_{dl})^{1/2} \quad (19c)$$

$$f_b/f_{min} = K^o_b (a_2''')^{-1} (D)^{1/2} \quad (20a)$$

$$= (C^o_{dl}/C^o_c)^{1/2} (D)^{1/2} \quad (20b)$$

Inspection of Eq. (16)-(20) shows that R_{po} and f_b both depend on the ratio ρ/d. On the other hand, f_b/f_{min} and Φ_{min} depend only on D. The result that f_b/f_{min} (Fig. 9 d) shows different dependence on exposure time for CR#2 on the one hand and CR#1 and 5 on the other hand, suggests that the coating degradation process is different for these two groups of coating systems. For CR#1 and 5 one can conclude that the observed decrease of R_{po} (Fig. 8b) and the increase of f_b (Fig. 9a) are due mainly to a decrease of the coating resistivity ρ. The most likely sequence of events for CR#2 is the following. In the first two months of exposure the coating resistivity ρ decreased and a very small delaminated area A_d developed (Fig. 8 and 9). The large increases of f_b (Fig. 9b) and C_{dl} (Fig. 8c) and the large decrease of R_{po} (Fig. 8b) after 100 d are due to an increase of A_d and the appearance of a large blister from which rust spots emerged. Eventually this blister was broken and evidence of delamination around the blister was observed visually. The continuous increase of f_b/f_{min} is therefore due to an increase of D. Since Φ_{min} had already reached very low values (1°-2°) it was not sensitive enough to document the increasing value of D between 100 and 300 d.

Inspection of the time dependence of the ratios R_1 and R_2 confirms that coating degradation was the largest for CR#2 followed by CR#1 and #5 (Fig. 10). It will be noted that R_2 is much less than the value for a perfect coating even at the beginning of the exposure. For CR#5, the initial R_2-values were only about as compared with the theoretical value of 2.

Obviously for these alkyd-based coatings some conducting paths were already existing in the as-received condition or were formed immediately after immersion.

For the same samples which were exposed after a small defect was applied, the impedance is dominated by the reactions in the defect which represents a low-resistance path. Therefore, parameters such as f_b, f_{min} and Φ_{min} (Fig. 14) cannot be used to evaluate coating deterioration. However, it is in principle possible to obtain information concerning coating delamination originating from the defect based the analysis of the EIS-data. For the data shown in Fig. 13, it is difficult the obtain such information since C_{dl} for CR#5 shows a very sharp increase in the first days of exposure (Fig. 13 b), while R_p remains more or less constant (Fig. 13 c). On the other hand, R_p decreases continuously for CR#1 and 2, while C_{dl} remains more or less constant. Since both parameters depend on A_d (Eq. 2 and 3), one would expect that they show similar changes with time.

The samples which had been exposed for two years in Florida were also exposed in the as-received condition and after application of a small artificial defect. However in the latter case, a cathodic potential of-1250 mV vs SCE was applied in order to determine the relative resistance of these coatings to delamination. In examining the results of the analysis of the EIS-data one finds a very large increase of C_c for CR#2 which is due to water uptake of the coating (Fig. 16a). For the same coating without outdoor exposure a much smaller water uptake was observed (Fig. 8 a). A decrease of R_p (Fig. 16b) and an increase of f_b (Fig. 16c) were only observed for CR#2 in the exposure time of 55 d. A comparison of the changes of f_b, f_{min}, tan Φ_{min} and f_b/f_{min} for CR#2 in Fig. 18 shows that f_b increases in a much shorter time to high frequencies after outdoor exposure. Since Φ_{min} and f_b/f_{min} , which are independent of ρ (Eq. 19 and 20), also show significant changes with time, one can conclude that for CR#2 which had been exposed outdoors for two year both D and ρ change during testing in NaCl. As mentioned above several rust spots had developed under blisters for this coating system.

The time dependence of R_1 and R_2 (Fig. 17) confirms that rapid coating degradation occurred for CR#2 with both R_1 and R_2 showing a continuous decrease with time. For CR#3 a large drop of R_2 occurred in the first 14 d, but then R_2 increased again. The time dependence of R_1 and R_2 for CR#6, 7 and 9 suggests that these are very stable coating systems.

In the cathodic delamination tests only CR#1, 2, 3 and 4 showed significant delamination. The largest effect occurred for CR#3 (alkyd/

enamel alkyd) which had not been tested without outdoor exposure. This result suggests that the alkyd-based coating systems are more susceptible to delamination than the other systems tested in this study. Fairly good agreement was obtained between the EIS-data (C_{dl}, R_{po}), the current density at -1250 mV and visual observation after the pull-test.

5.2 Outline of the Design of a Coating Monitor

A number of parameters have been identified in this project which can be used to detect and quantify coating damage. These parameter include f_b, f_{min}, f_b/f_{min}, Φ_{min}, R_1 and R_2. Since these parameters are determined in the high frequency region for sample which show significant coating deterioration, their measurement can be performed accurately in a very short time period. An instrument, which determines coating damage based on f_b, f_{min}, Φ_{min}, R_1 and R_2 would determine impedance data starting at 10-100 kHz, scan to lower frequencies and stop the measurement when the parameter of interest has been detected.

The proposed measurement principle can be illustrated for the data obtained for the as-received samples and those which were tested after outdoor exposure. Assuming that a decision has been made that the lowest frequency to be measured by a coating monitor is 100 Hz, coating damage would first be indicated after about 100 d for the as-received CR#2. At this time f_b has exceeded 100 Hz for the first time. If such a monitor would not only determine f_b, but also f_{min} and Φ_{min}, readings would be obtained for all three parameters at this time. For CR#1 and 5 readings for the three parameters would be first obtained after 245 d and 280 d, respectively. Recording of three parameters plus calculation of f_b/f_{min} would make the coating monitor more reliable.

A coating monitor based on the ratios R_1 and R_2 would also give a signal pointing to coating degradation for CR#1, 2 and 5 . Assuming that it has been decided that damage is indicated when R1 drops below 1.25 and R2 drops below 1.0, a signal would be received for CR#1 after about 50 d for R_2 and after about 300 d for R_1. For CR#2 signals would be recorded after 70 d and 130 d. CR#5 is a difficult case, since the first measurement already results in R_1 being close to 1.0 and R_2 never dropping below 1.25. For the samples which were tested for 55 d after outdoor exposure, damage would be indicated for CR#2 after 12 d (R2) and 30 d (R1). The only other sample for which the monitor would provide a signal would be CR#3 for which R_2 drops below 1.0 after about 8 d, but then increases again after 20 d. Since the measurement of R_1 and R_2 was carried out during the entire test period in laboratory experiments, this anomalous

behavior has been detected. In field testing, a misleading signal might be recorded if damage assessment is based only on R_2.

The coating monitor could be designed similar to the barnacle electrode for the measurement of hydrogen in steel (8,9). A cylindrical magnet could house in a plastic body the electrochemical cell which consists of a steel counter electrode and a sponge with a gel electrolyte. Since the cell is housed in the magnet, it can be attached to steel structures in any direction. EIS-data would be collected at zero applied potential between the coated sample and the steel counter electrode using either existing equipment such as the Schlumberger potentiostat and frequency response analyzer which were used in this study or equipment especially designed for the polymer coating monitor.

6.0 Summary and Conclusions

1. Nine different coating systems on cold rolled steel have been tested by recording of EIS-data during immersion in 0.5 N NaCl (open to air). One set of samples has been tested in the as-received condition and after application of an artificial defect. Another set was tested after outdoor exposure for two years at Cape Canaveral, Florida. For this set the susceptibility to cathodic delamination was also evaluated.

2. For the set which was tested in the as-received condition for one year, the sample with an all-latex coating was eliminated from further testing since the coating was so porous that the impedance spectra resembled those usually found for bare steel. In long term testing, coating damage was observed only for the alkyd/enamel (CR#1), the alkyd/enamel Si-alkyd (CR#2) and the zinc-rich primer/epoxy polyamide/polyurethane (CR#5) systems.

3. For the set which was tested for 55 d after outdoor exposure significant coating damage could be detected only for CR#2. In the cathodic delamination tests the largest damage occurred for the alkyd/enamel alkyd (CR#3) system. Delamination was also observed for CR#1, 2 and 4, which are all alkyd-based coatings.

4. A theoretical analysis of the impedance of polymer coated steel has been performed with the goal of identifying parameters which could be used in the design of a coating monitor. The results of this analysis suggest that the breakpoint frequency f_b and the frequency f_{min} of the phase angle minimum Φ_{min} observed at high frequencies are suitable for

this purpose. These parameters can be determined at relative high frequencies which reduces the measurement time greatly. The analysis also showed that f_b and f_{min} depend both on the delaminated area A_d and the coating resistivity ρ, while Φ_{min} and the ratio f_b/f_{min} depend only on A_d. Recording of f_b, f_{min} and Φ_{min} allows therefore to determine coating damage and to assess the extent of coating delamination at the metal/coating interface. The recording of the impedance at two frequencies can also give information concerning coating degradation if one frequency is chosen in the region where the impedance can be expected to remain capacitive and the other frequency is chosen in the region where resistive components appear as the coating experiences degradation.

5. The design of a commercial coating monitor could be based on f_b, f_{min} and Φ_{min} or the frequency ratios R_1 and R_2. This monitor could consist of a cylindrical magnet housing the electrochemical cell which consists of a bare steel electrode and a gel electrolyte in a sponge. EIS-data can be recorded for the coated steel - bare steel couple at various locations of a painted steel structure. Starting from very high frequencies (> 10 kHz) impedance data can be recorded until a phase angle of 45° is determined (f_b) or a minimum of the phase angle is recorded (f_{min}, Φ_{min}). Using suitable calibration charts, which can be established based on theoretical and experimental data, a qualitative assessment of coating damage can be made. It can then be decided whether the paint should be stripped and the steel structure should be repainted.

7.0 References

1. F. Mansfeld, M. W. Kendig and S. Tsai, Corrosion 38, 478 (1982)

2. M. W. Kendig, F. Mansfeld and S. Tsai, Corr. Sci. 23, 317 (1983)

3. F. Mansfeld and M. W. Kendig, ASTM STP 866, 122 (1985)

4. S. Haruyama, M. Asari and T. Tsuru, in "Corrosion Protection by Organic Coatings", The Electrochem. Soc., Proc. Vol. 87-2, p. 197 (1987)

5. F. Mansfeld, C. H. Tsai and H. Shih, "Determination of Coating Delamination and Corrosion Damage with EIS", in Proc. Symp. "Advances in Corrosion Protection by Organic Coatings", The Electrochem. Soc., Proc. Vol. 89-13, p. 228 (1989)

6. F. Mansfeld and C. H. Tsai, "Determination of Coating Delamination with EIS; I. Basic Considerations", Corrosion (in press)

7. F. Mansfeld and C. H. Tsai, "Determination of Coating Delamination with EIS; II. Development of a Method for Field Testing of Protective Coatings", to be submitted to Corrosion

8. U. S. Patent 4,221,651

9. D. A. Berman, J. J. DeLuccia and F. Mansfeld, Metal Progress 115, 58 (1979)

8.0 Figure Captions

Fig. 1. Equivalent circuit for the corrosion behavior of a polymer coated metal.

Fig. 2. Theoretical impedance plots for D = 10^{-4} (1), 10^{-3} (2), 10^{-2} (3), 10^{-1} (4) and 1 (5) and different coating thicknesses d = 10 μm (Fig. 2a), 100 μm (Fig. 2b), and 1000 μm (Fig. 2c); A = 32 cm2.

Fig. 3. Dependence of Φ_{min}, f_{min} and f_b on D for three coating thicknesses.

Fig. 4. Theoretical plot of R_1 and R_2 versus delamination ratio D for a coating thickness d = 10 μm.

Fig. 5. Electrochemical cell for impedance measurements with a reference electrode (RE), a counter electrode (CE) and a polymer coated working electrode (WE).

Fig. 6. Experimental approach for recording of EIS-data.

Fig. 7. Impedance spectra for CR#2 after (a) 43 days , (b) 90 days, and (c) 162 days

Fig. 8. Analysis of EIS-data for coatings CR#1, 2, 5, 6, and 9 as a function of exposure time; (a) C_c , (b) R_{po} ,(c) C_{dl} and (d) R_p.

Fig. 9. Time dependence of the parameters f_b , f_{min}, Φ_{min}, and f_b/f_{min}.

Fig. 10. Time dependence of R_1 and R_2 for (a) CR#1, (b) CR#2, (c) CR#5, (d) CR#6, and (e) CR#9.

Fig. 11. Impedance spectra for samples with an artificial defect after 24 h (Fig. 11 a and b) and 44 d (Fig. 11 c and d) immersion in 0.5 N NaCl.

Fig. 12. Time dependence of E_{corr} for samples with an artificial defect.

Fig. 13. Time dependence of (a) R_h, (b) C_{dl} and (c) R_p for samples with an artificial defect.

Fig. 14. Time dependence of (a) f_{min} and (b) Φ_{min} for samples with an artificial defect.

Fig. 15. Impedance spectra for samples after outdoor exposure and immersion in 0.5 N NaCl for 24 h (Fig. 15 a and b) and 30 d (Fig. 15 c and d)

Fig. 16. Time dependence of coating capacitance C_c (Fig. 16a), polarization resistance R_p (Fig. 16b) and breakpoint frequency f_b during exposure to 0.5 N NaCl for coated steel samples after outdoor exposure.

Fig. 17. Time dependence of R_1 and R_2 during exposure to 0.5 N NaCl for coated steel samples after outdoor exposure

Fig. 18. Time dependence of f_b, f_{min}, Φ_{min} and f_b/f_{min} for coating system CR#2.

Fig. 19. Impedance spectra for CR#1 with cathodic polarization at E_{SCE} = -1250 mV for (a) 1 h, (b) 6 h and (c) 24 h.

Fig. 20. Time dependence of the polarization current at E_{SCE} = -1250 mV.

Fig. 21. Time dependence of (a) R_h, (b) C_{dl} and (c) R_p for cathodically polarized CR#1, 2, 3, 4, 5, 6, 7, and 9.

Fig. 22. Comparison of the calculated A_d-values with A_d determined from the tape pull test for CR#1, 2, 3, and 4.

Fig. 1

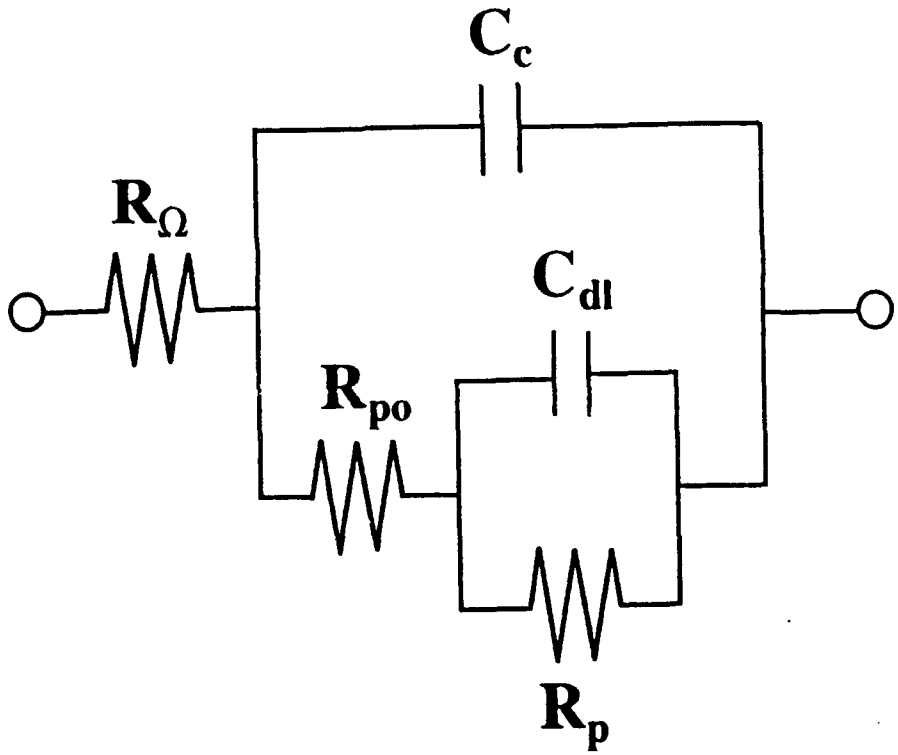

Fig. 2a

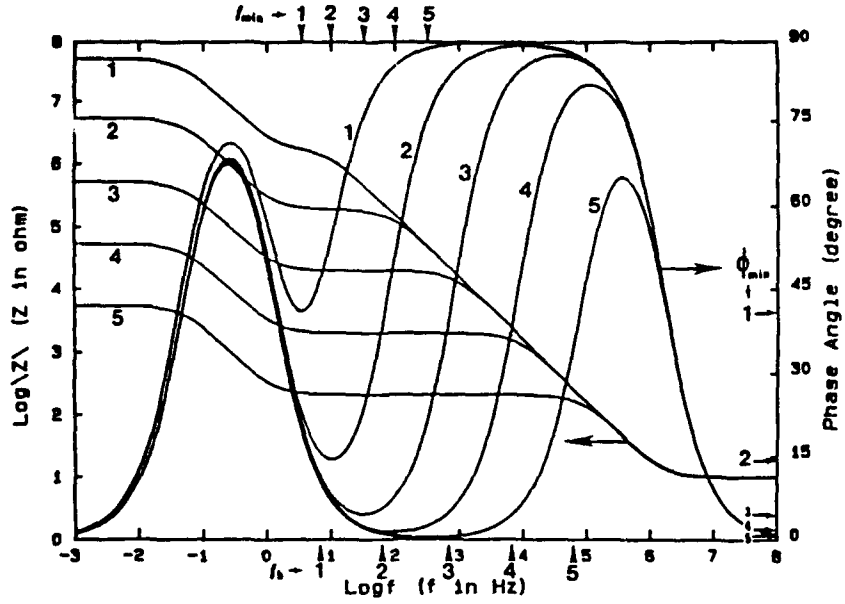

Fig. 2b

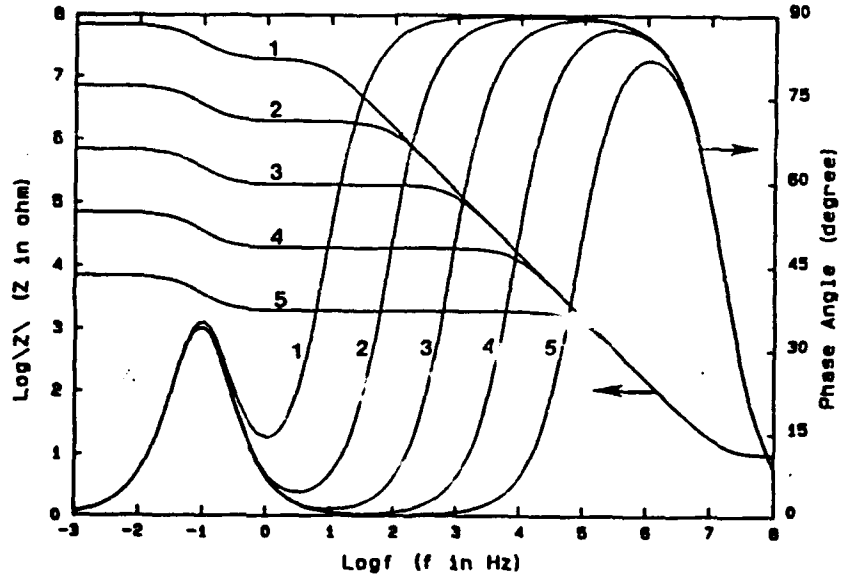

Fig. 2c

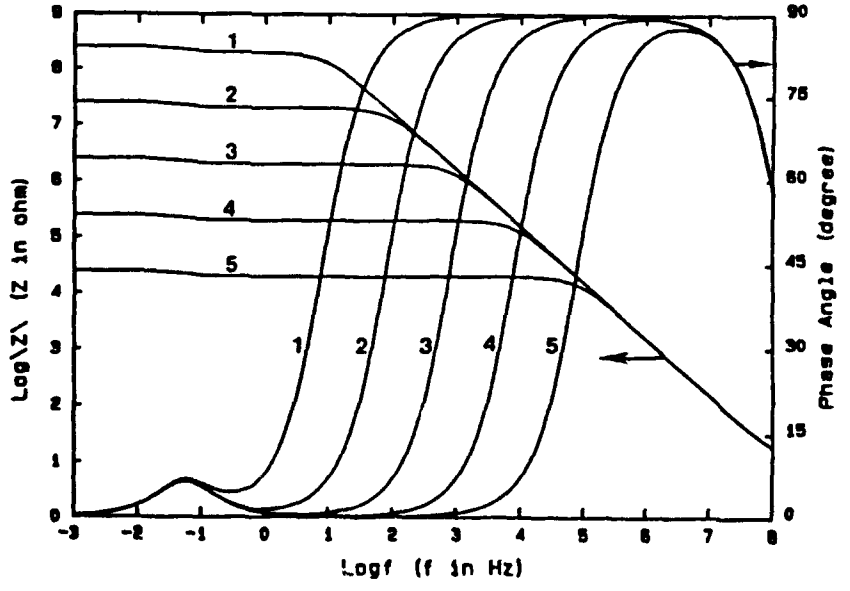

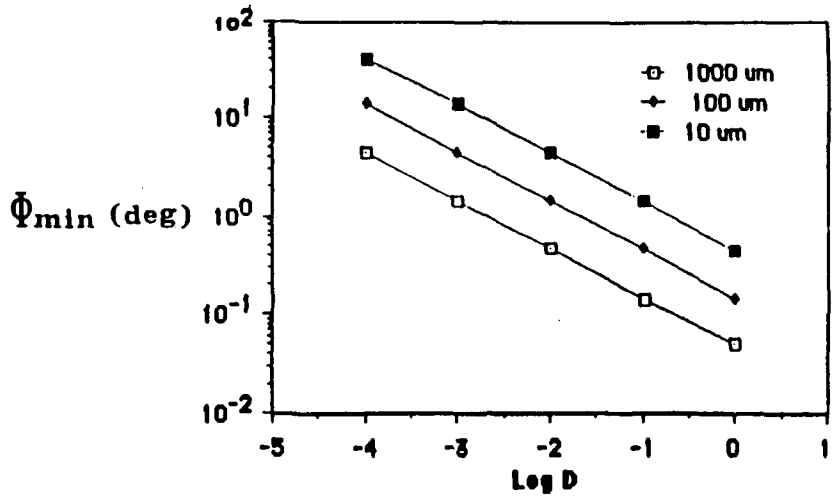
Φ_{min} (deg)
10^2
10^1
10^0
10^{-1}
10^{-2}
1000 um
100 um
10 um
-5
-4
-3
-2
-1
0
1
Log D

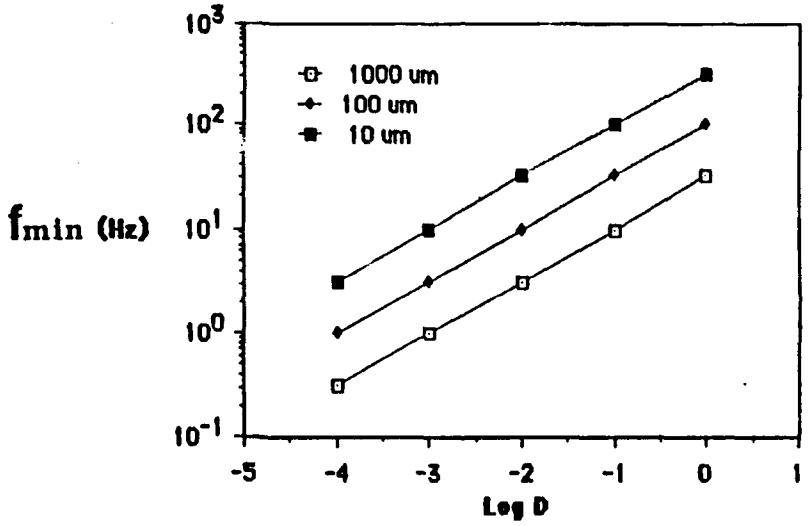
f_{min} (Hz)
10^3
10^2
10^1
10^0
10^{-1}
1000 um
100 um
10 um
-5
-4
-3
-2
-1
0
1
Log D

Fig. 3

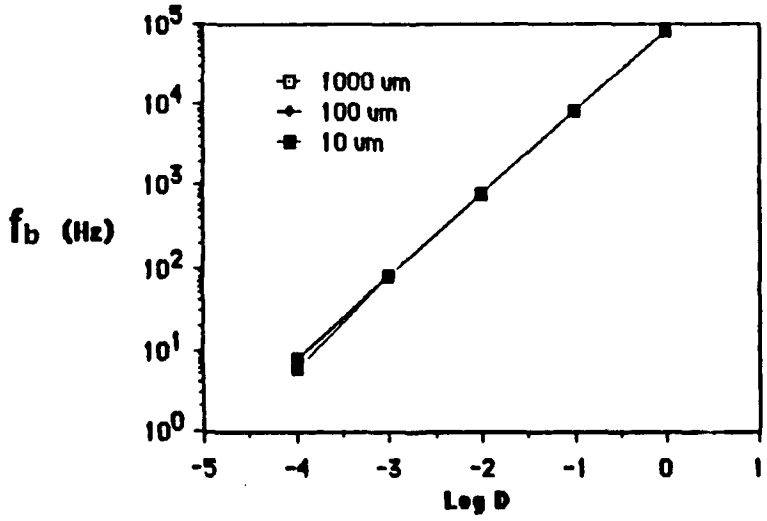
f_b (Hz)
10^5
10^4
10^3
10^2
10^1
10^0
1000 um
100 um
10 um
-5
-4
-3
-2
-1
0
1
Log D

Fig. 4
Theorectical plot of R1 and R2 vs D
for Coating Thickness = 10 um

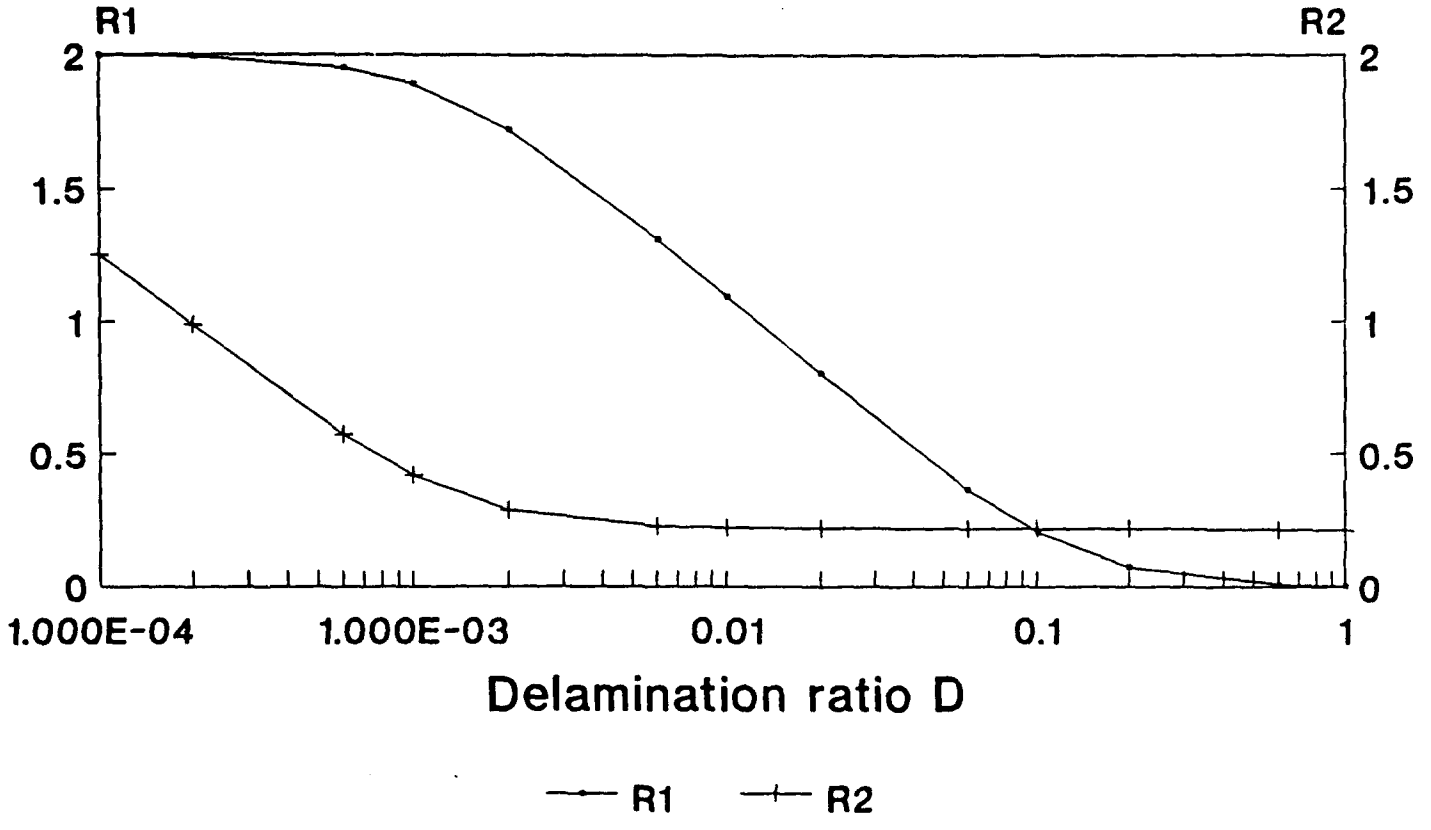

R1=log(Z100/Z10000), R2=log(Z1/Z100)

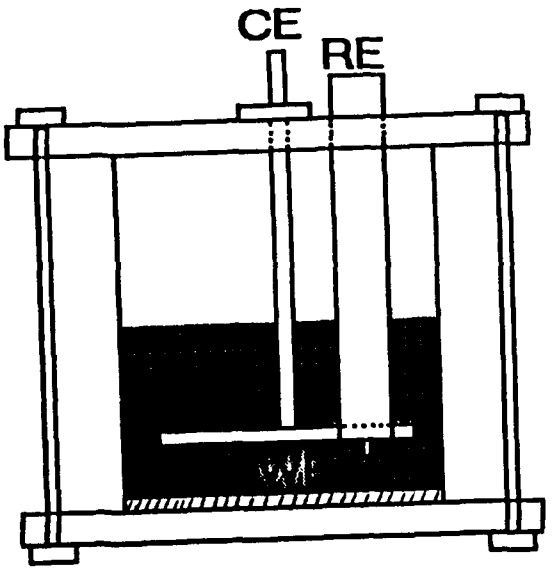
CE
RE

Fig. 5

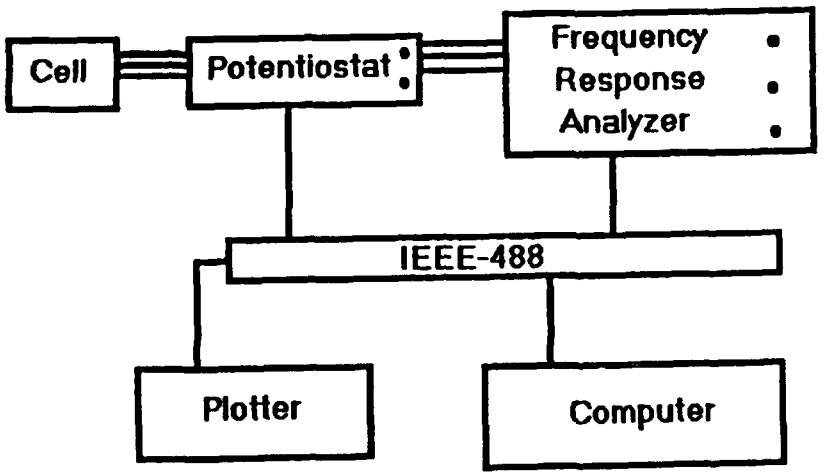
Cell
Potentiostat
Frequency
Response
Analyzer
IEEE-488
Plotter
Computer

Fig. 6

Fig. 7

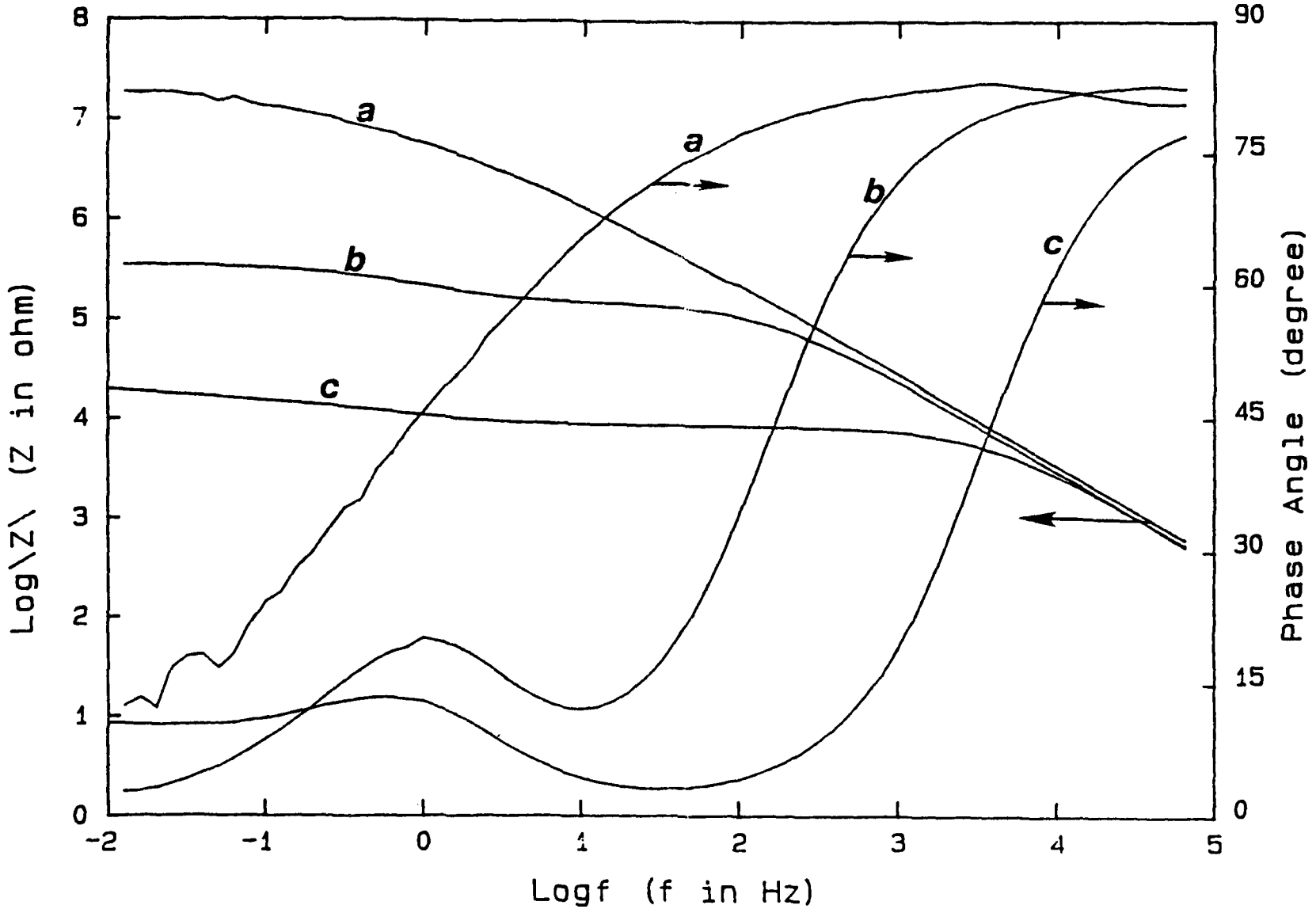
Log\Z\ (Z in ohm)
Phase Angle (degree)
Logf (f in Hz)
a
b
c
a
b
c
0
1
2
3
4
5
6
7
8
15
30
45
60
75
90
-2
-1
0
1
2
3
4
5

Fig. 8a
Capacitance vs Time for CR(1,2,5,6,9)

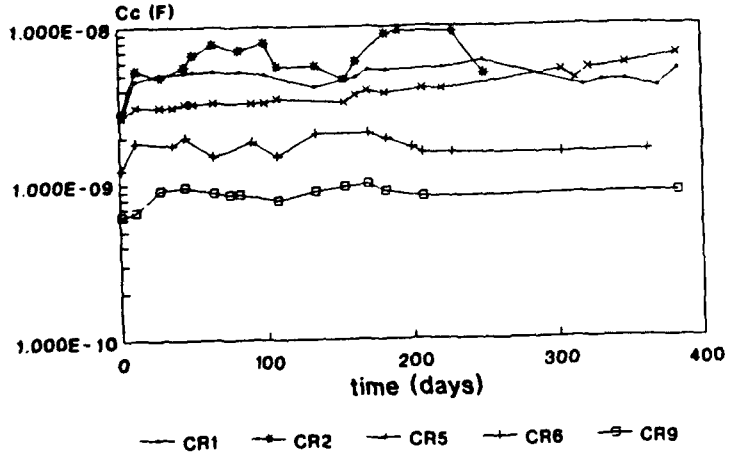

Fig. 8b
Rpo vs Time for CR(1,2,5)

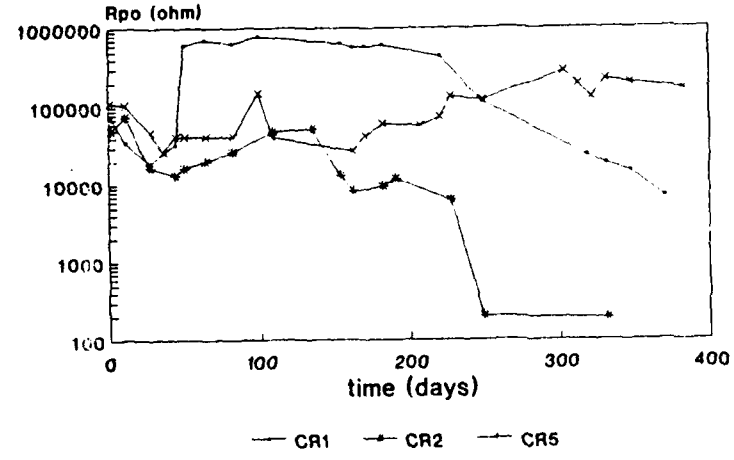

Fig. 8c
Cdl vs Time for CR(1,2,5)

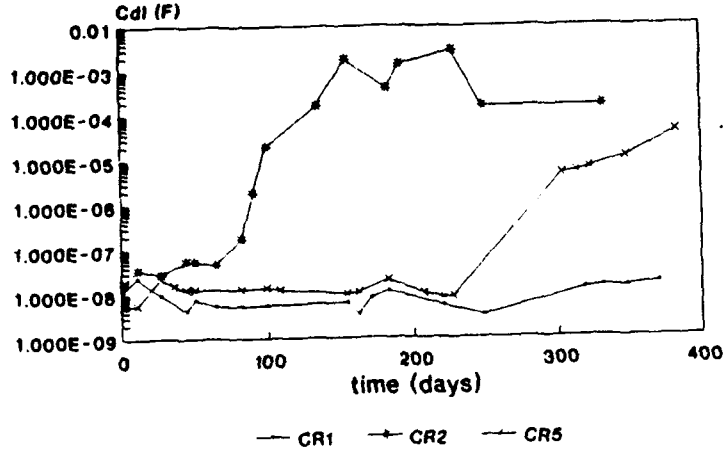

Fig. 8d
Rp vs Time for CR(1,2,5,6,9)

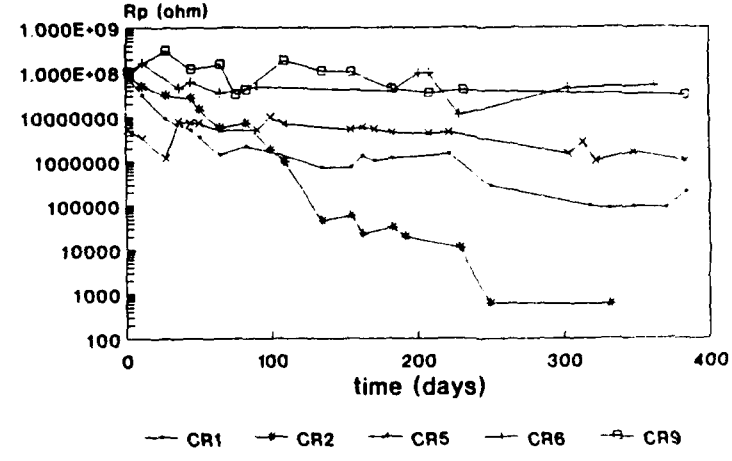

Fig. 9a
Breakpoint frequency vs time for
Sample CR(1,2,5,6,9)

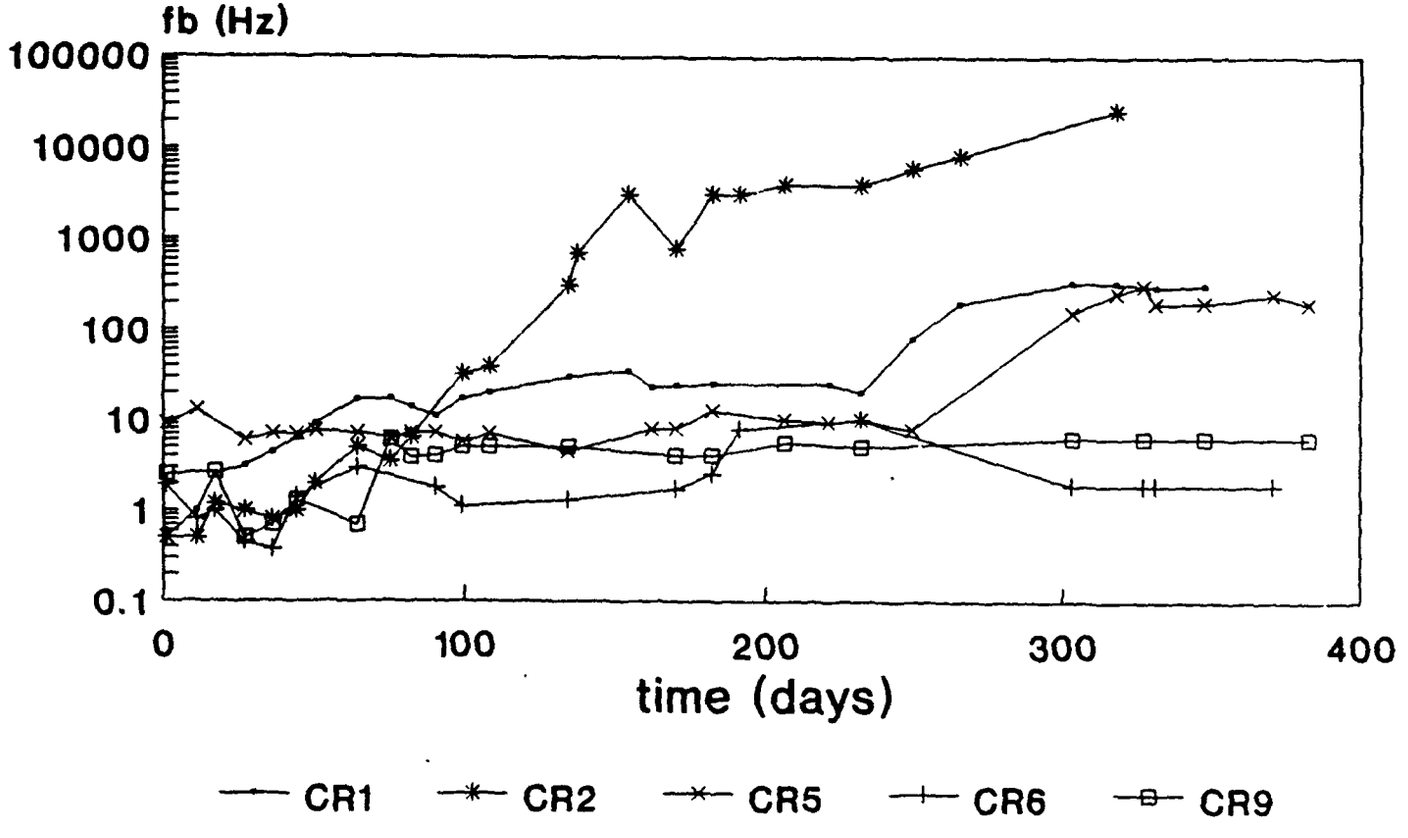

Fig. 9(b)

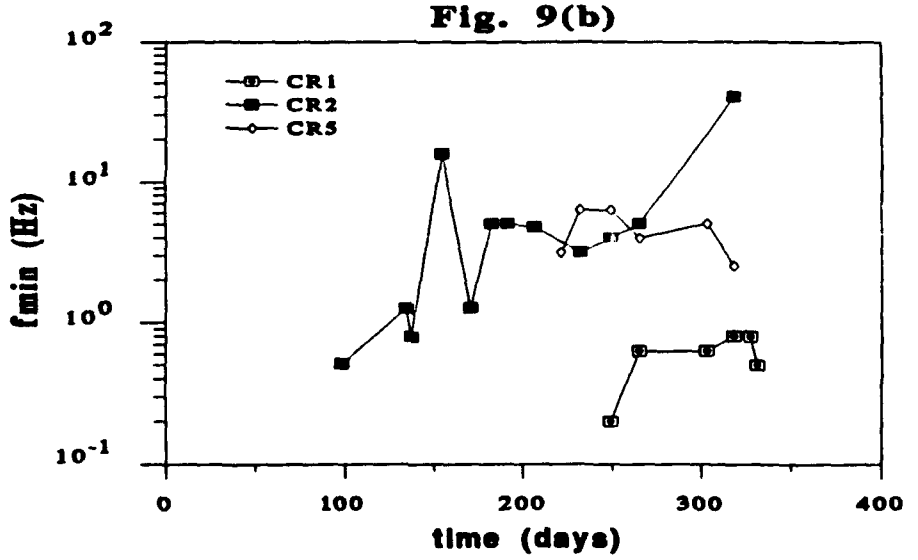

Fig. 9(c)

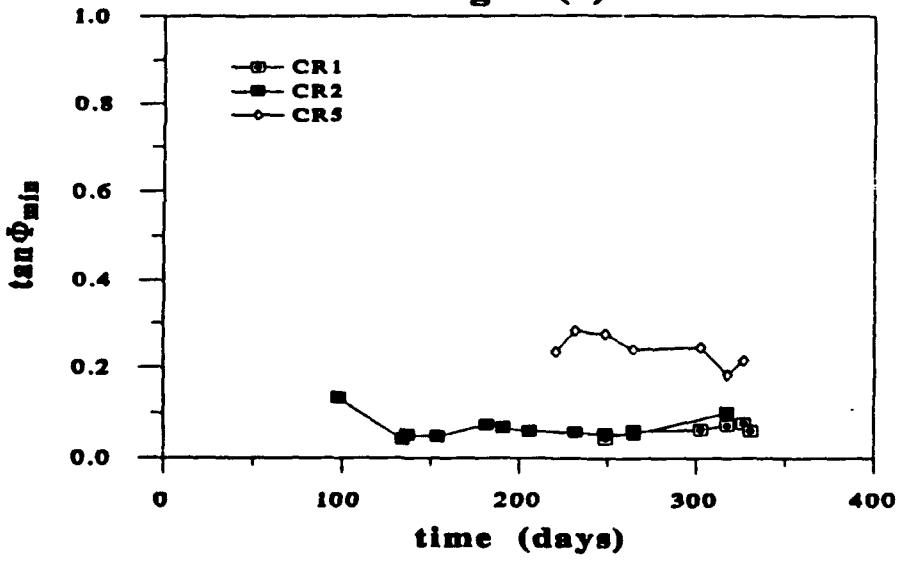

Fig. 9(d)

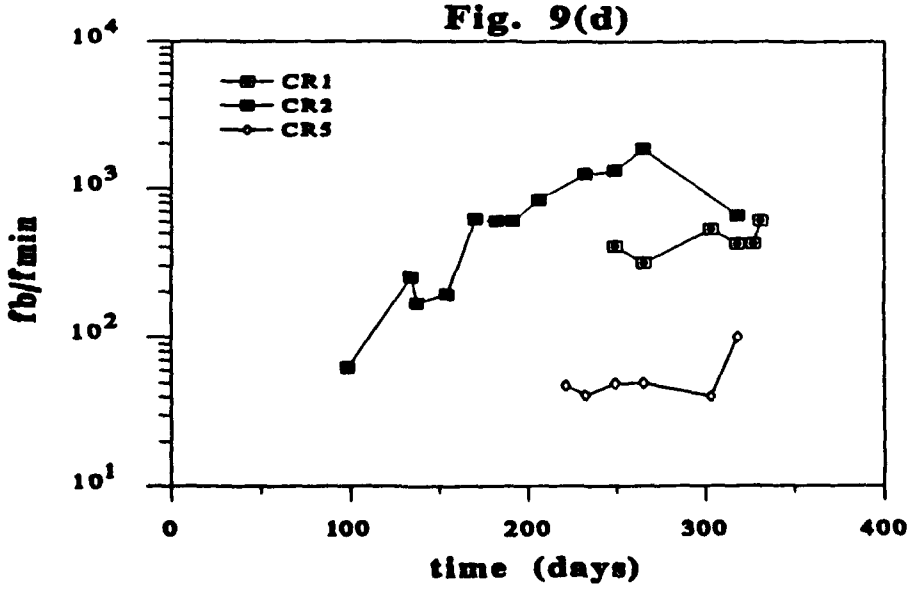

Fig. 10

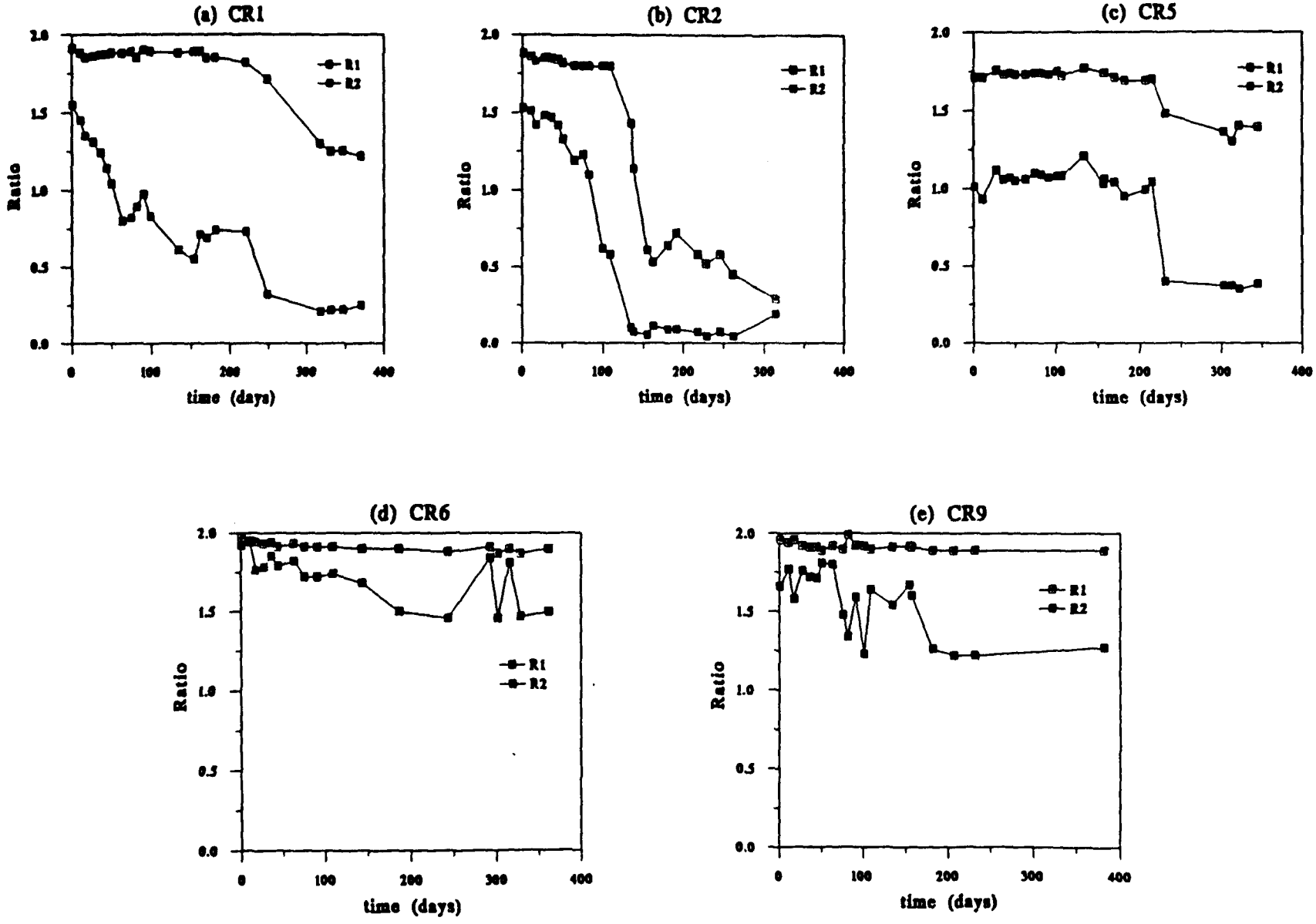
(a) CR1
(b) CR2
(c) CR5
(d) CR6
(e) CR9
Ratio
time (days)
R1
R2
0.0
0.5
1.0
1.5
2.0
0
100
200
300
400

Fig. 11a

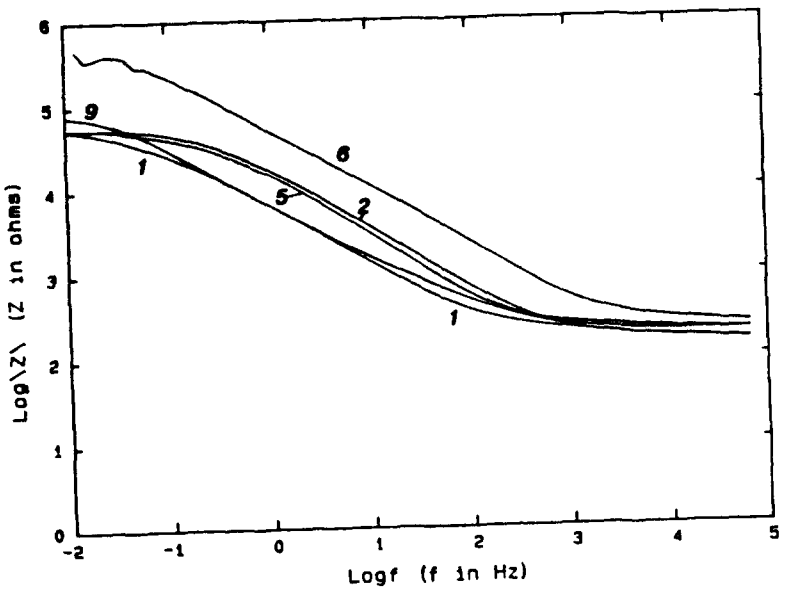

Fig. 11b

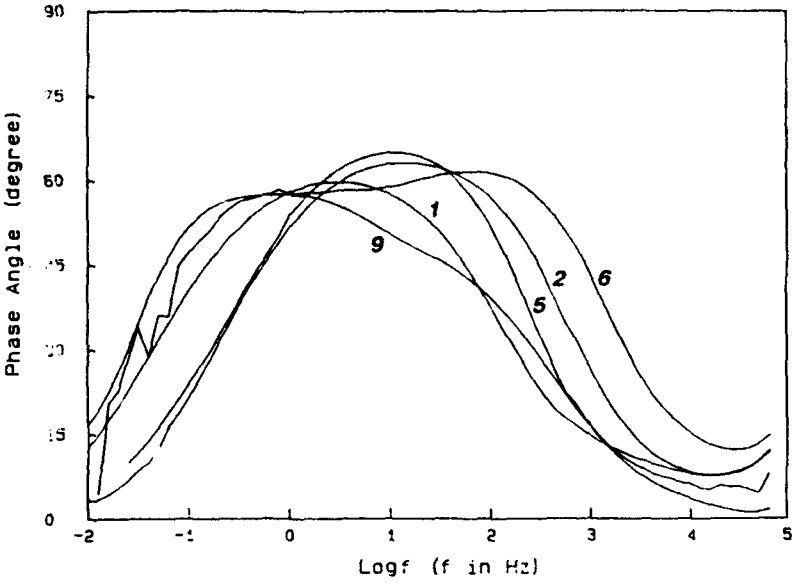

Fig. 11c

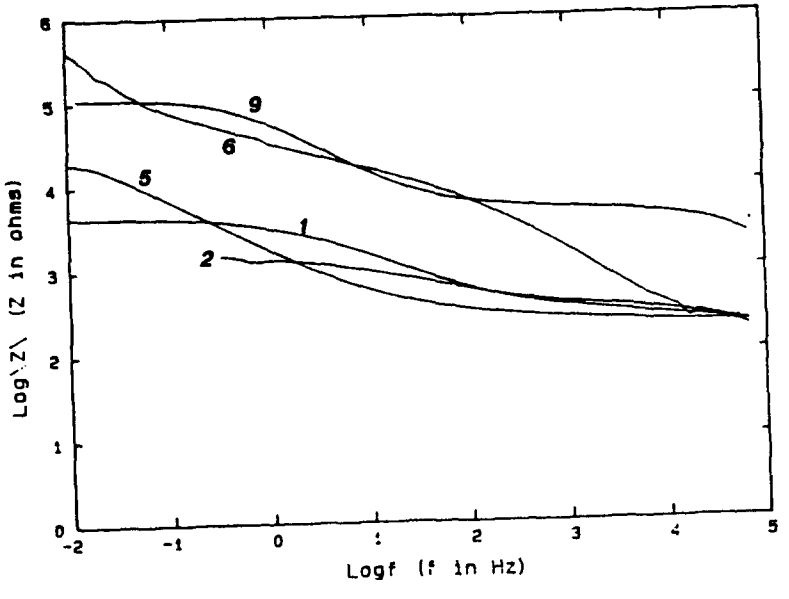

Fig. 11d

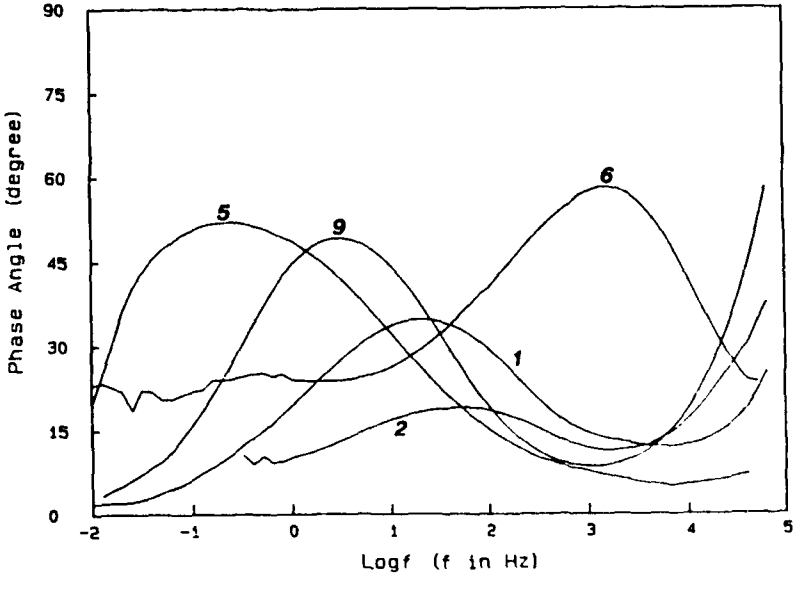

Fig. 12
Ecorr vs time for Coated Steel with an Artificial Defect (0.5 N NaCl)

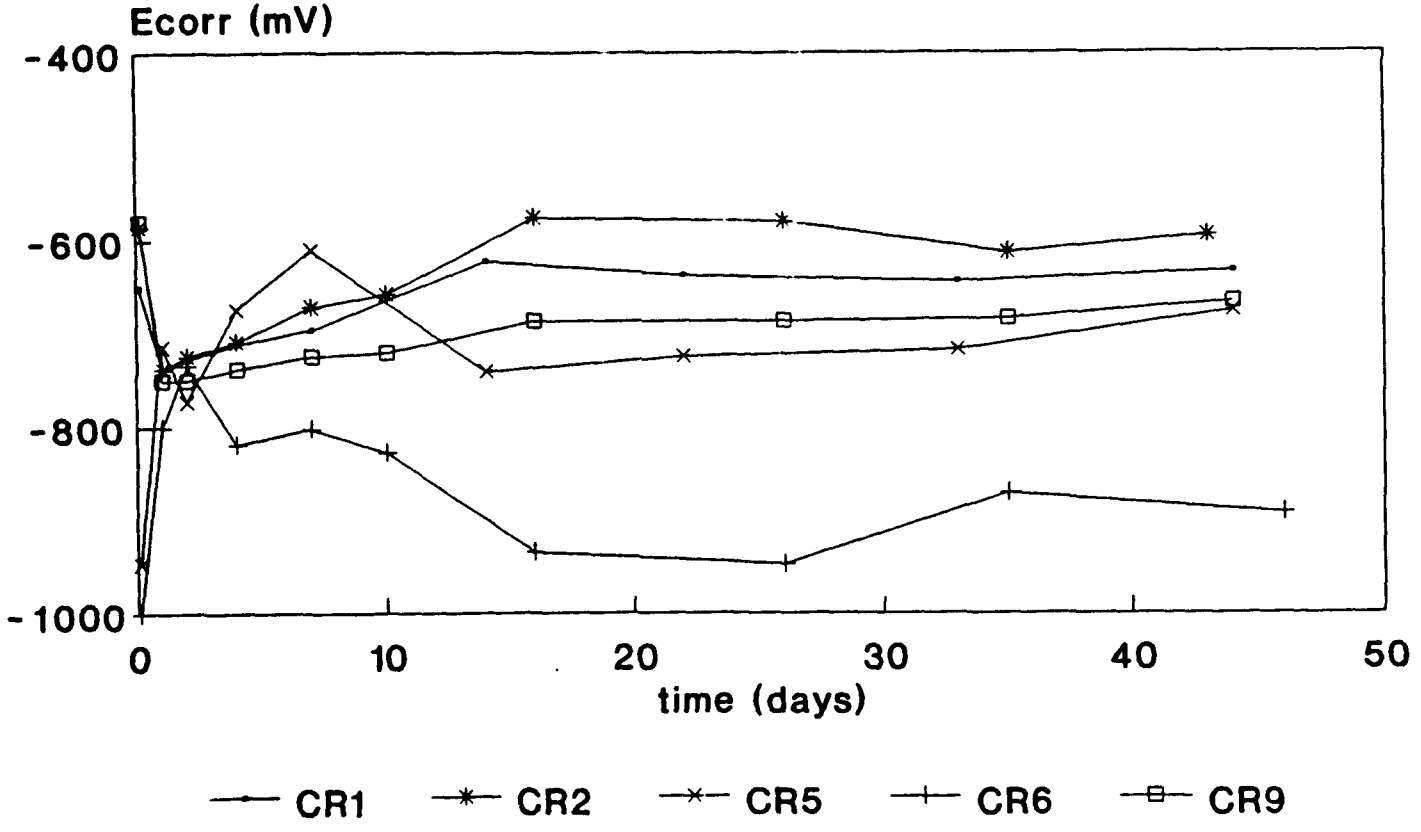

Fig. 13a
Rh vs Time for CR(1,2,5,6,9)
with an Artificial Hole

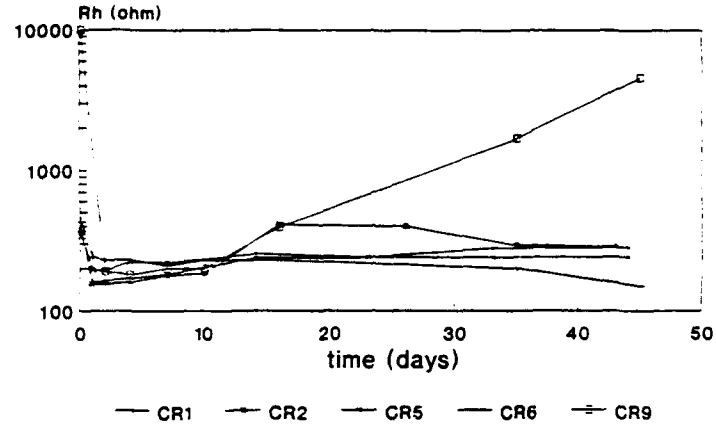

Fig. 13b
Cdl vs Time for CR(1,2,5,6,9)
with an Artificial Hole

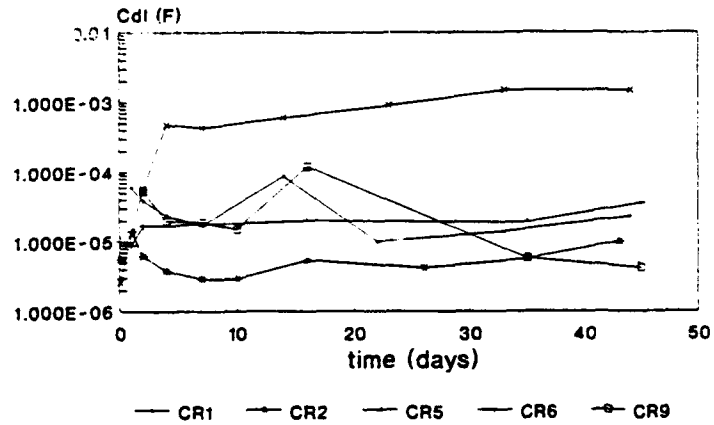

Fig. 13c
Rp vs Time for CR(1,2,5,6,9)
with an Artificial Hole

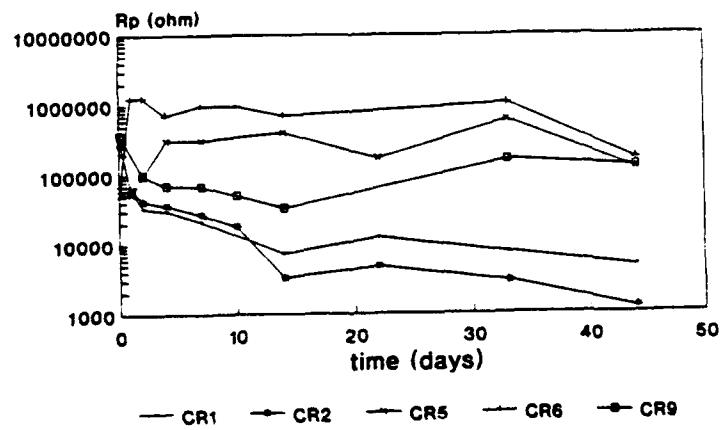

Fig. 14a
Frequency Minimum vs Time for
CR(1,2,5,6,9) with an Artificial Hole

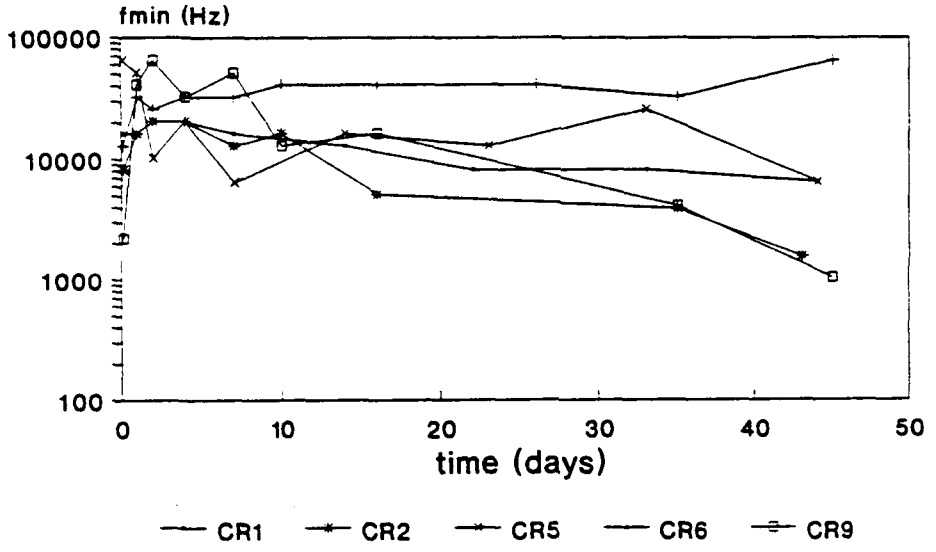

Fig. 14b
Phase Angle Minimum vs Time for
CR(1,2,5,6,9) with an Artificial Hole

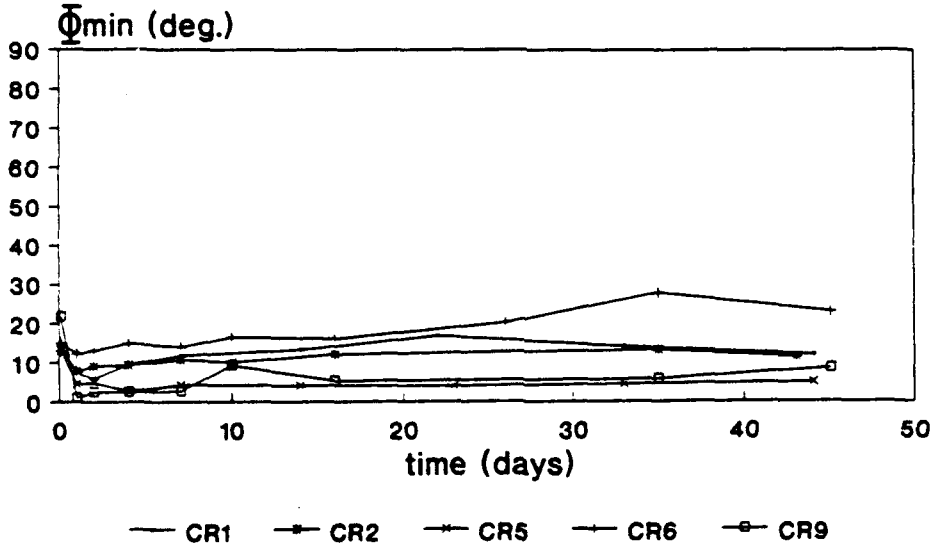

Fig. 15a

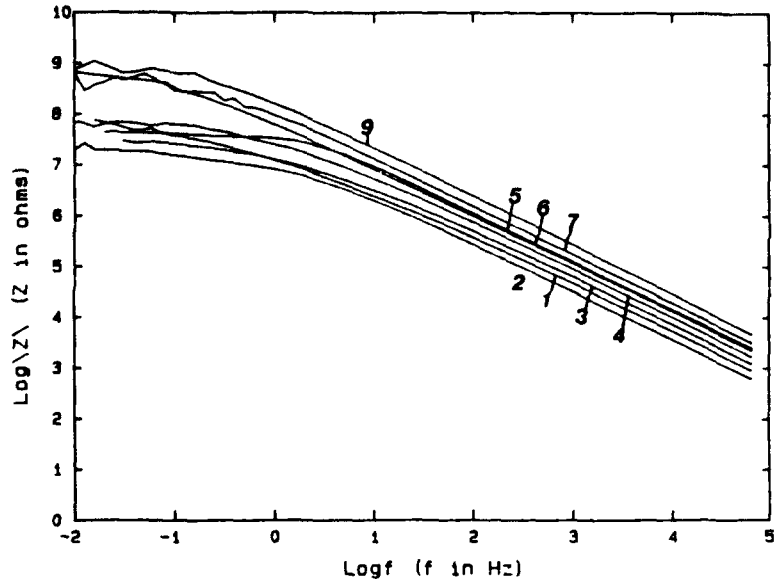

Fig. 15b

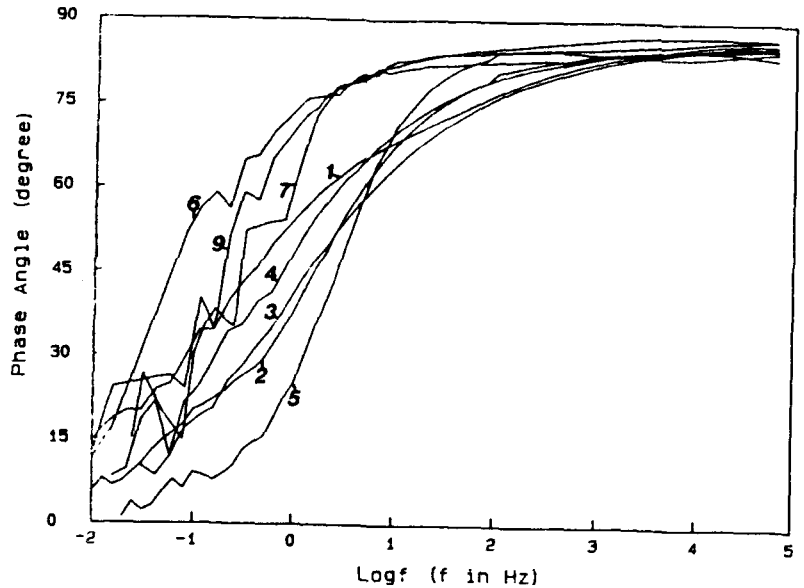

Fig. 15c

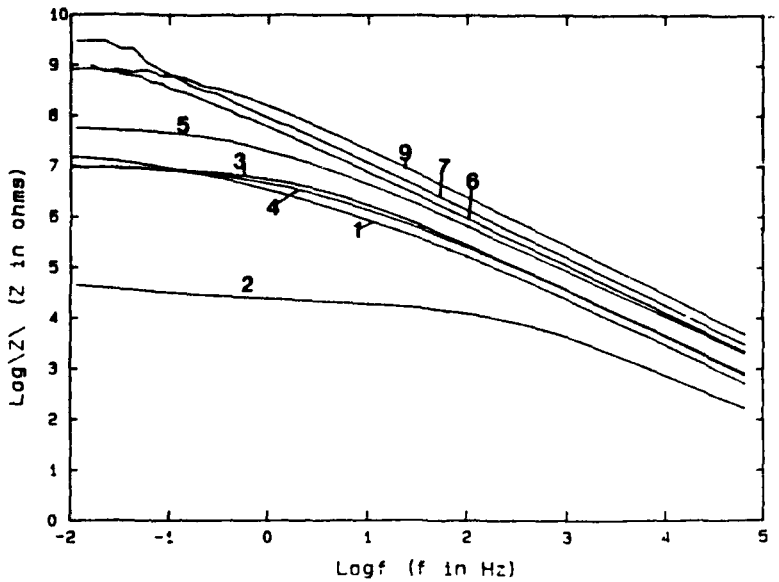

Fig. 15d

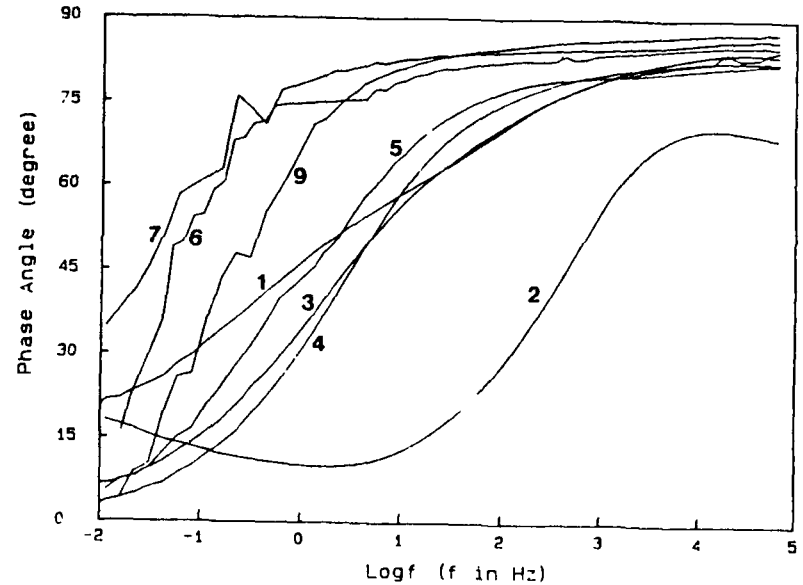

Fig. 16a

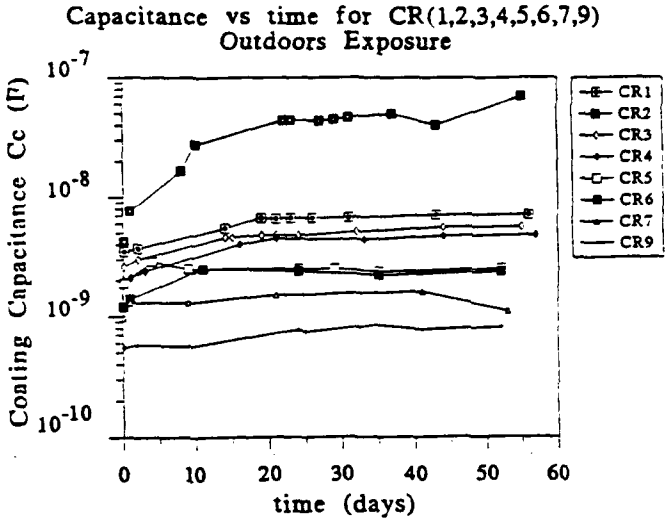

Fig 16b

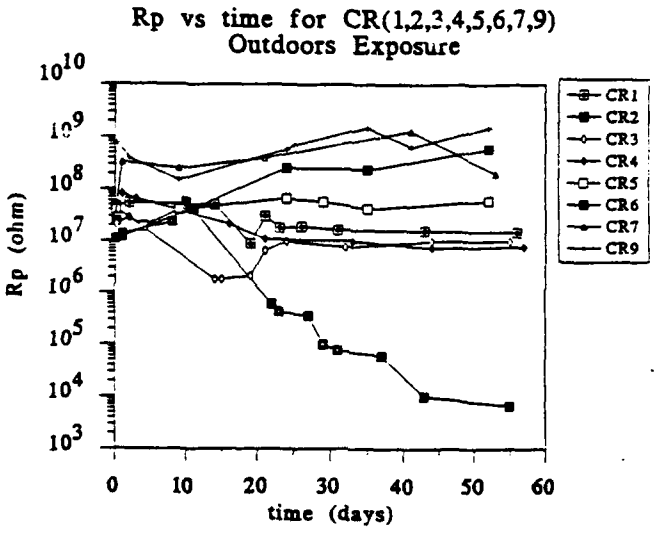

Fig. 16c

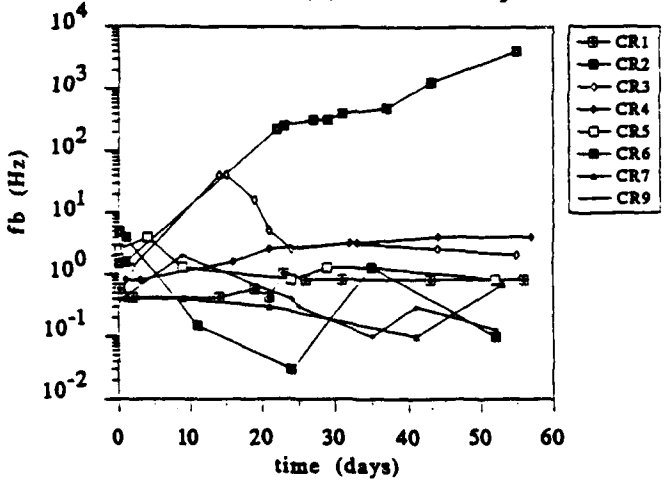

Fig. 17a

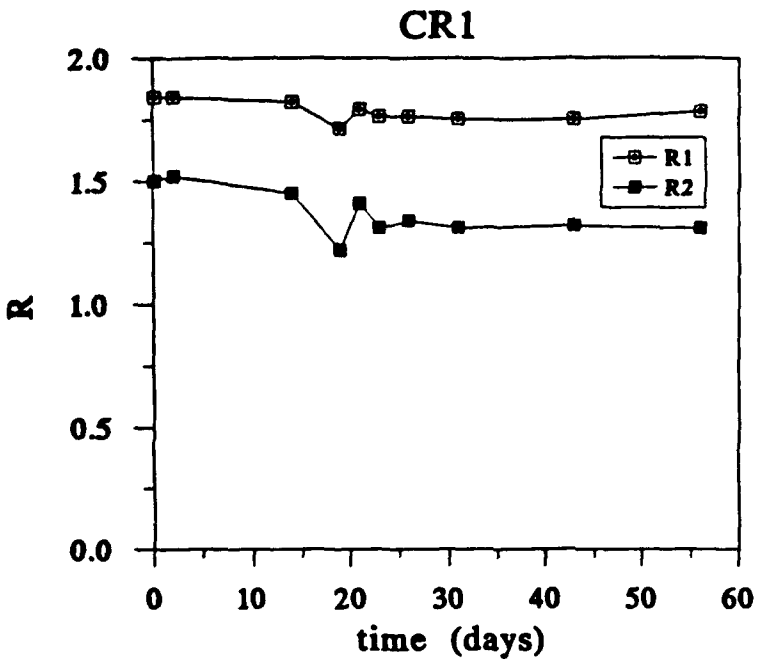

Fig. 17b

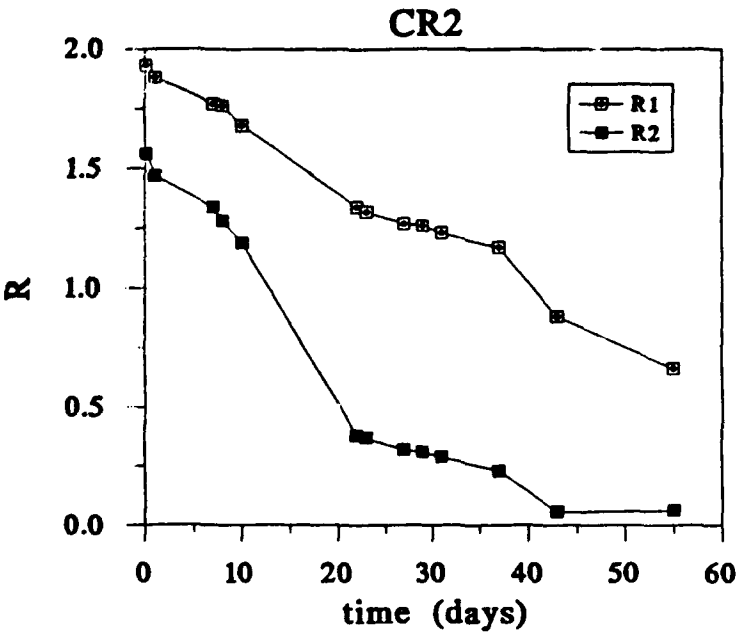

Fig. 17c

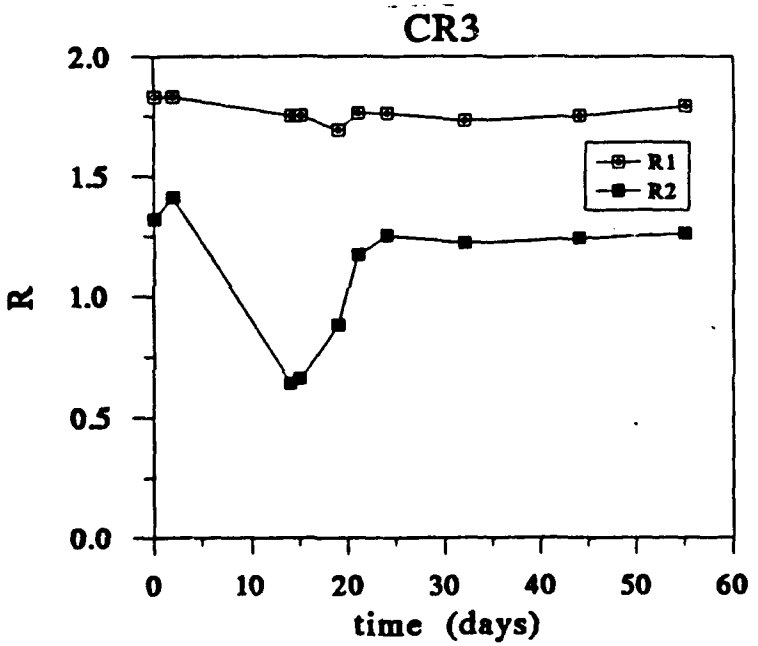

Fig. 17d

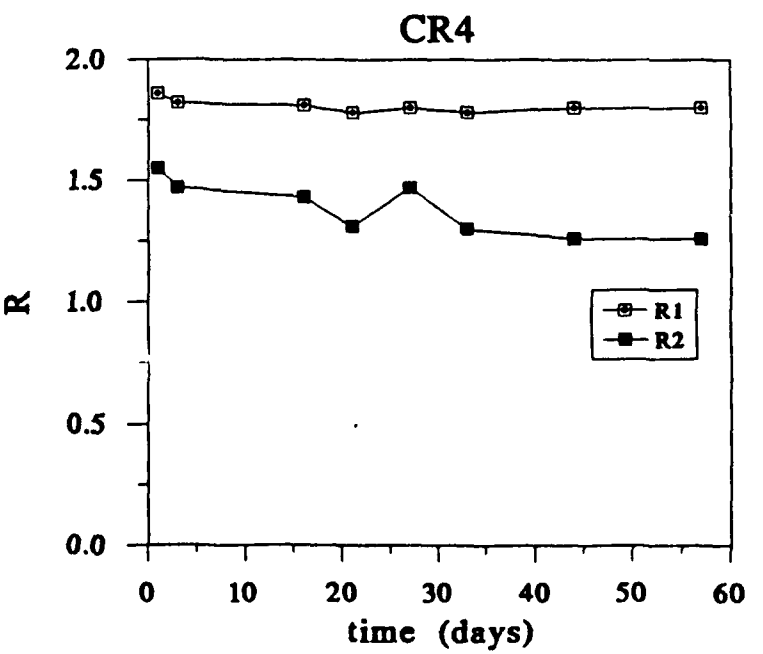

Fig. 17e

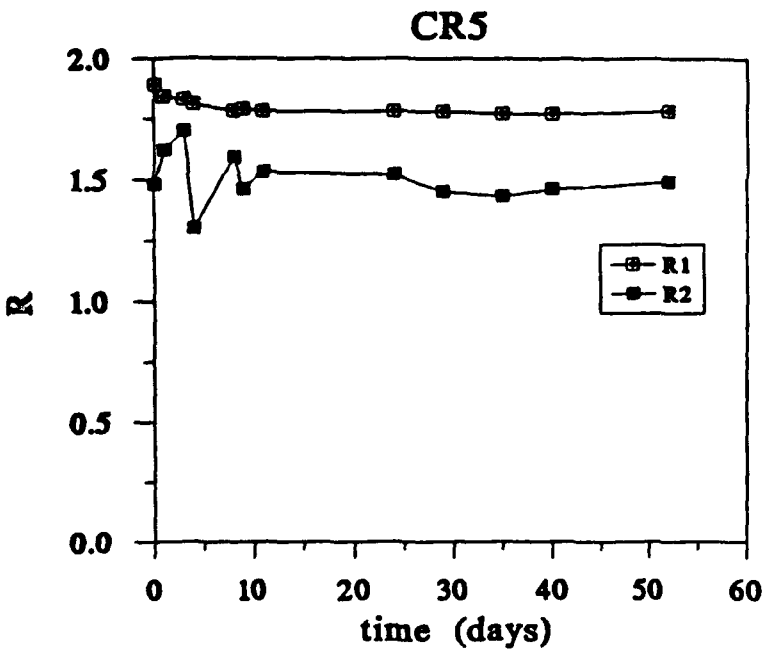

Fig 17f

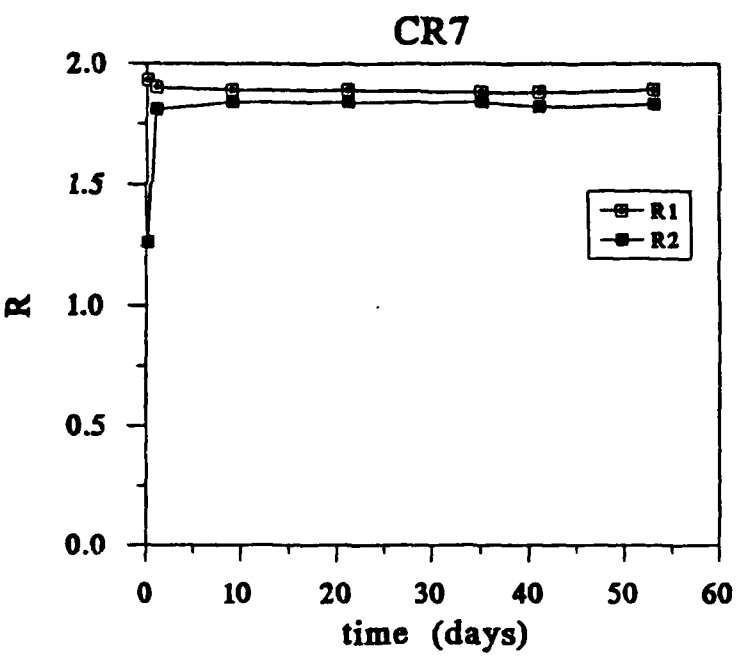

Fig. 17g

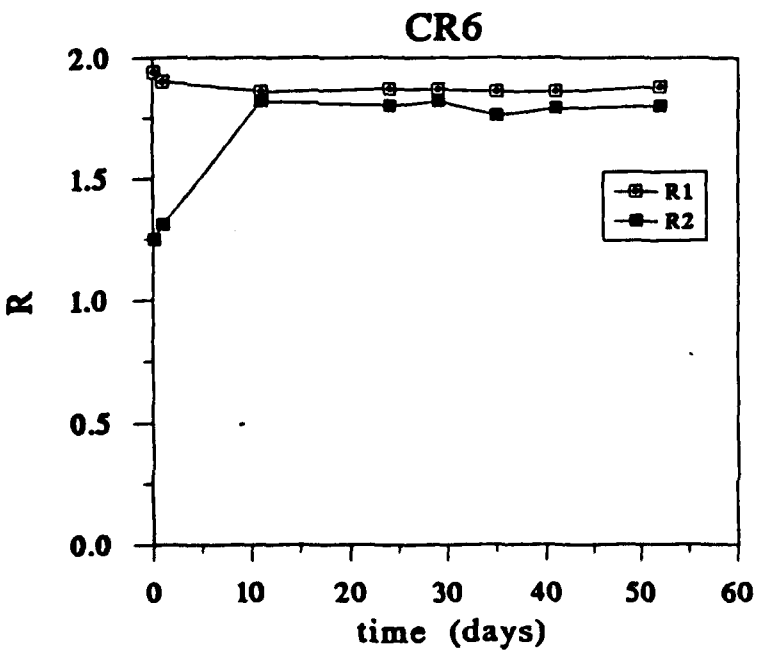

Fig. 17h

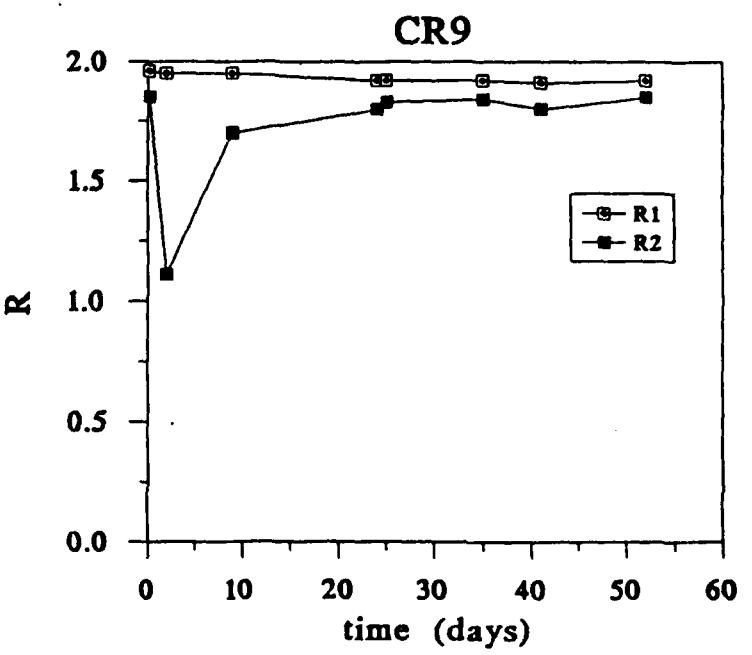

Fig. 18(a)

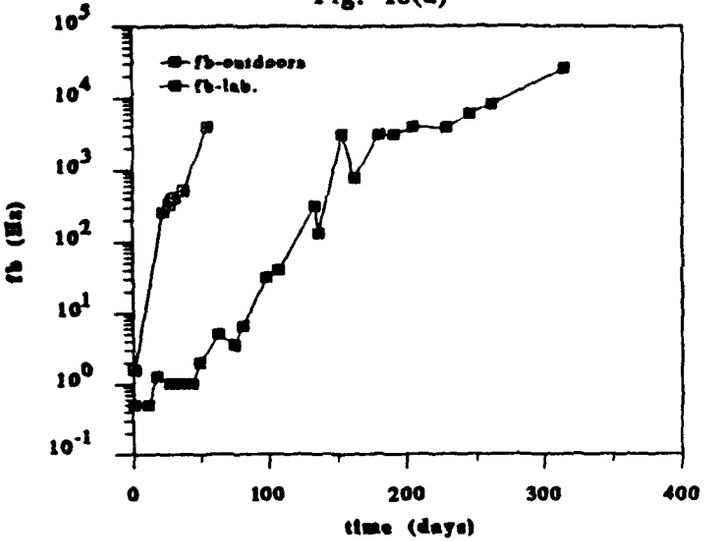

Fig. 18(b)

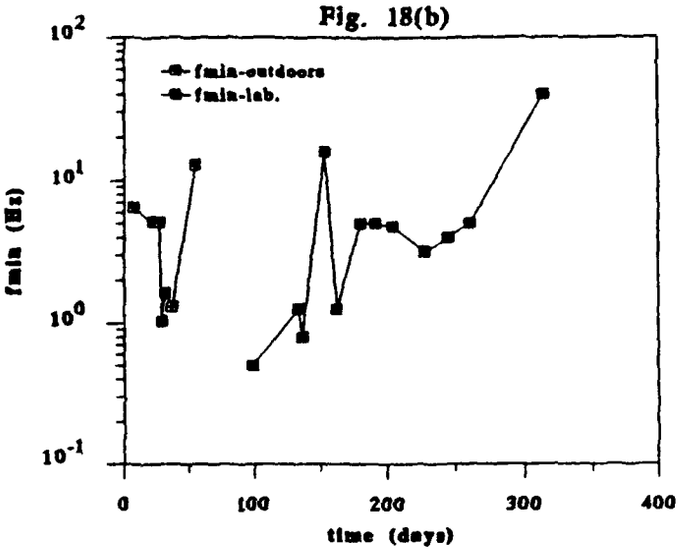

Fig. 18(c)

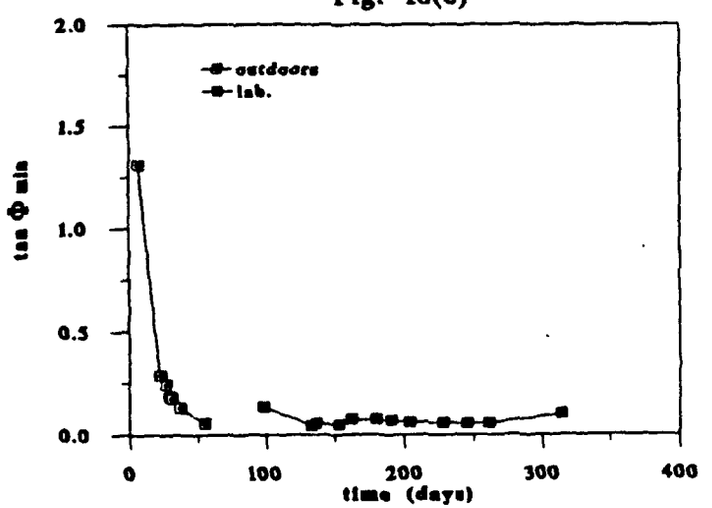

Fig. 18(d)

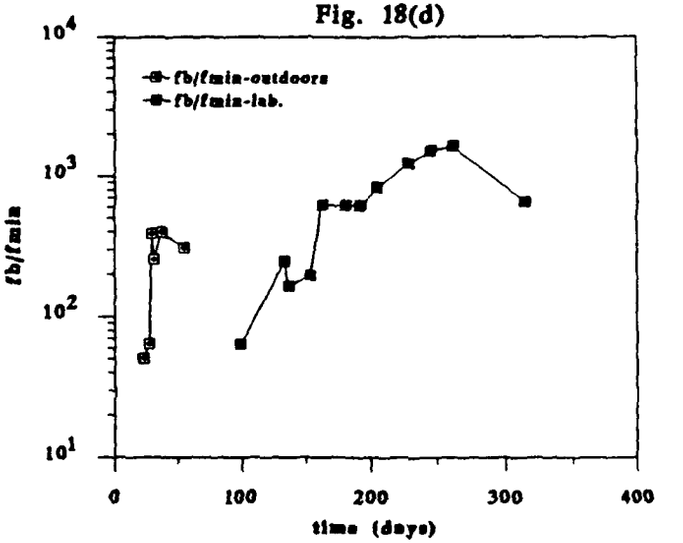

Fig 19

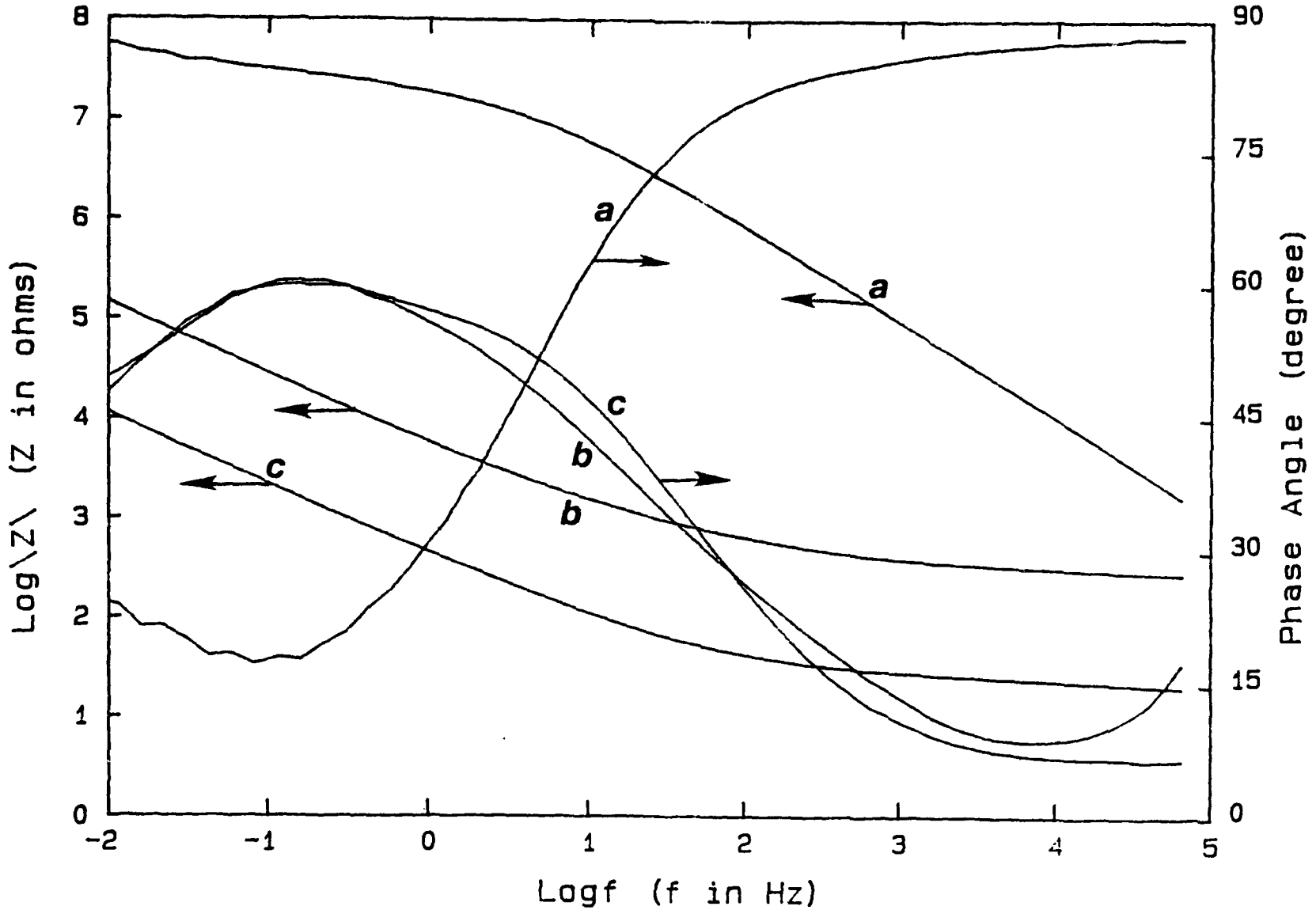
Log\Z\ (Z in ohms)
Phase Angle (degree)
Logf (f in Hz)
a
a
b
b
c
c
0
1
2
3
4
5
6
7
8
-2
-1
0
1
2
3
4
5
15
30
45
60
75
90

Fig. 20
Time dependence of Cathodic Current at
Esce = -1250 mV

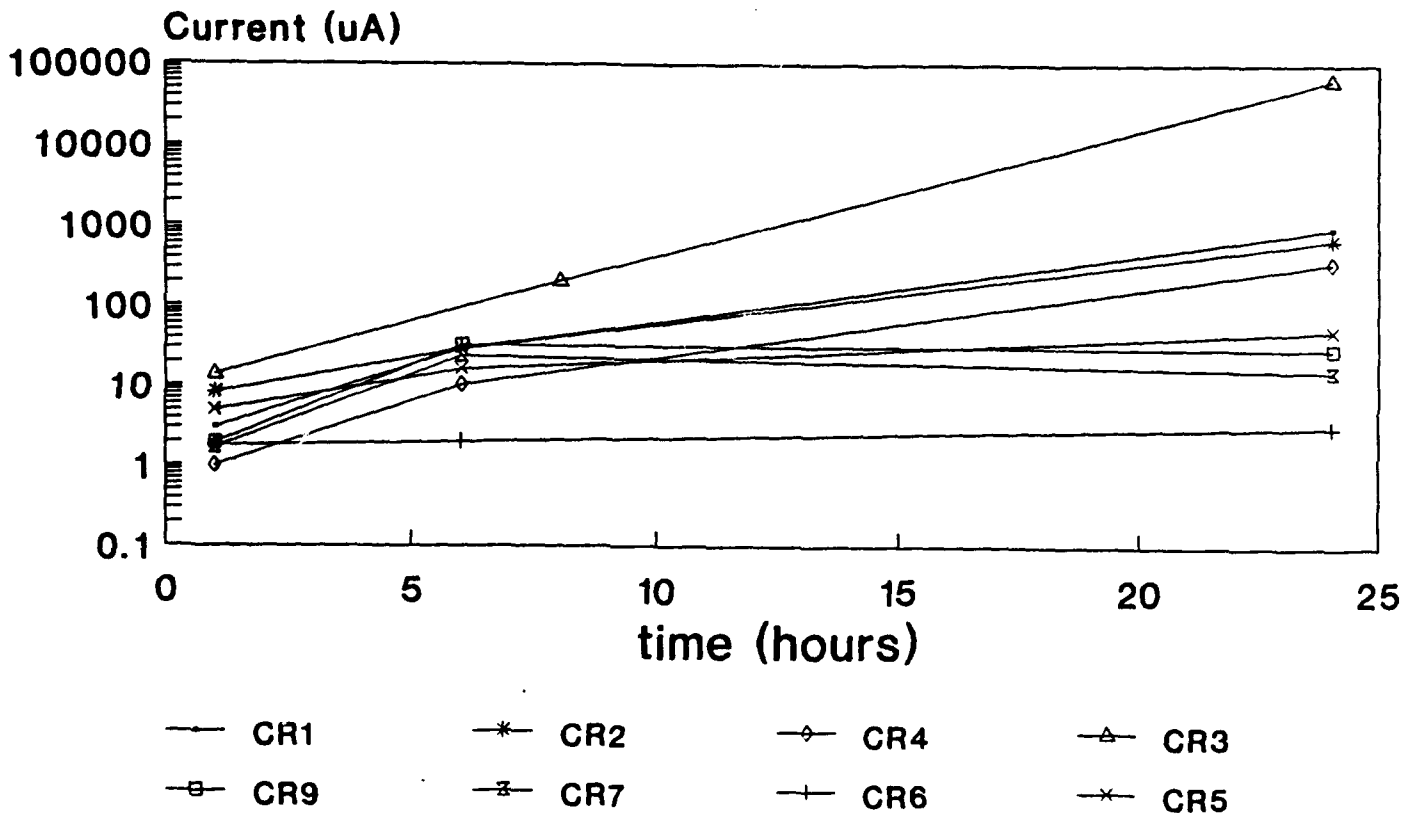

Fig. 21(a1)

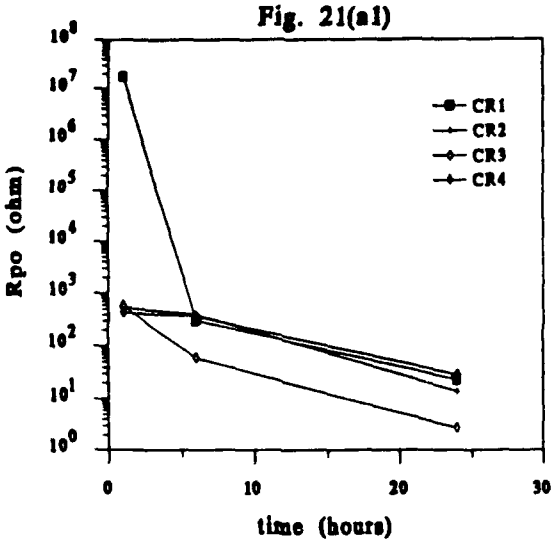

Fig. 21(a2)

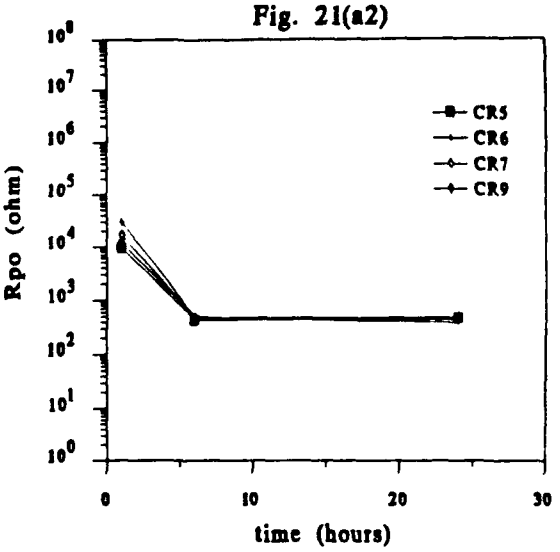

Fig. 21(b2)

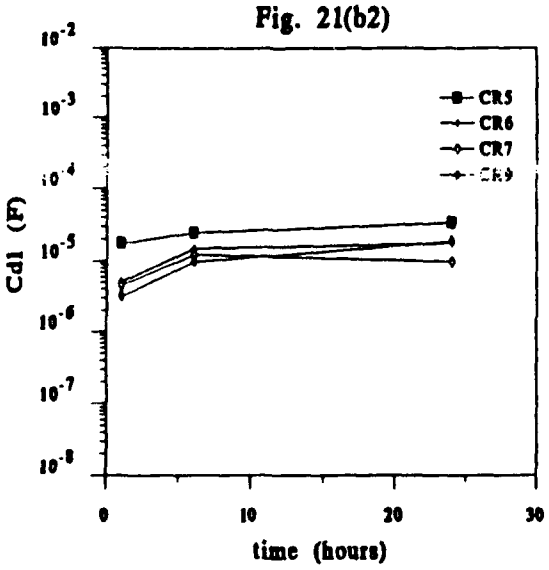

Fig. 21(b1)

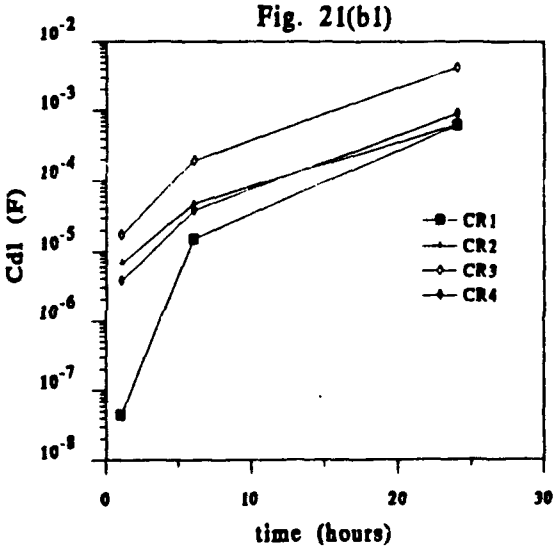

Fig. 21(c1)

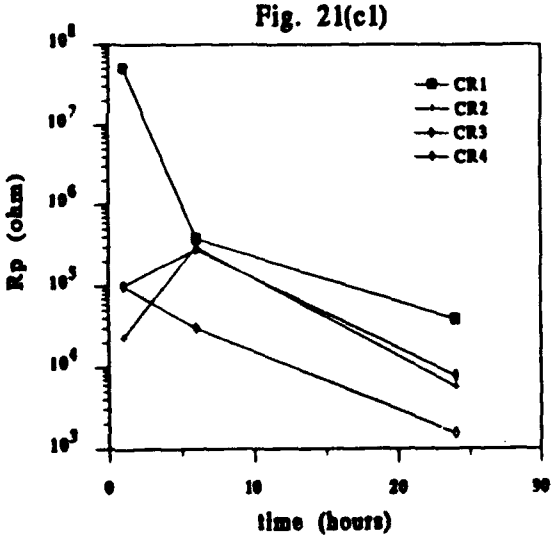

Fig. 21(c2)

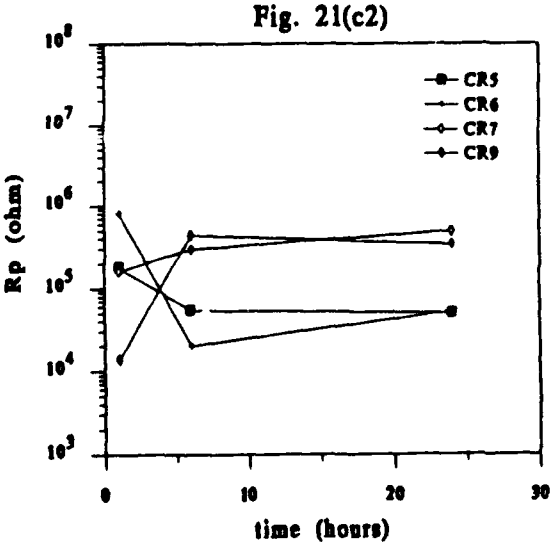

Fig. 22

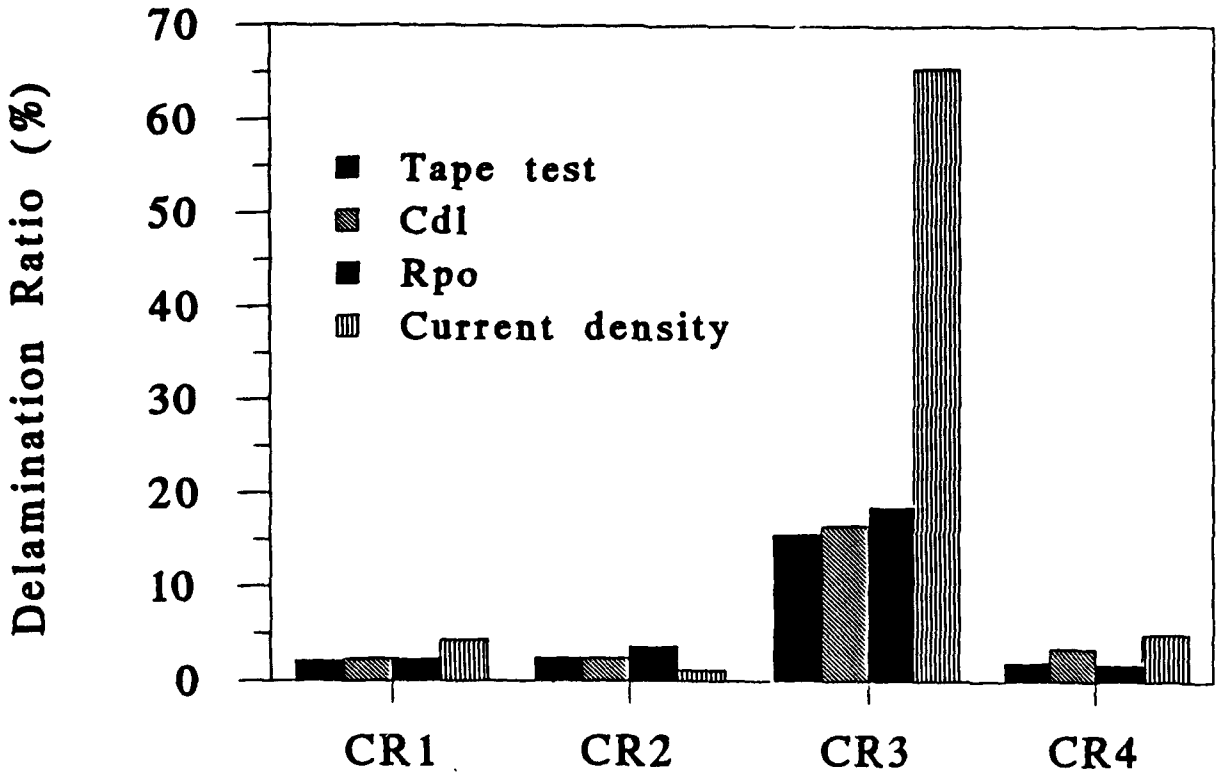
Delamination Ratio (%)
70
60
50
40
30
20
10
0
Tape test
Cdl
Rpo
Current density
CR1
CR2
CR3
CR4

DISTRIBUTION LIST

AFESC / TECH LIB, TYNDALL AFB, FL
AMERICAN CONCRETE / LIB, DETROIT, MI
APPLIED TECHNOLOGY AND MANAGEMENT / C. JONES, CHARLESTON, SC
ARCTEC, INC / CHES INSTRU DIV, TECH LIB, GLEN BURNIE, MD
ARMY / CH OF ENGRS, DAEN-CWE-M, WASHINGTON, DC
ARMY / CH OF ENGRS, DAEN-MPU, WASHINGTON, DC
ARMY CECOM R&D TECH LIBRARY / ASNC-ELC-I-T, FORT MONMOUTH, NJ
ARMY CERL / LIB, CHAMPAIGN, IL
ARMY ENGRG DIST / LIB, SEATTLE, WA
ARMY ENGRG DIST / LIB, PHILADELPHIA, PA
ARMY ENGRG DIST / LIB, PORTLAND, OR
ARMY EWES / LIB, VICKSBURG, MS
BABCOCK & WILCOX CO / TECH LIB, BARBERTON, OH
BATTELLE NEW ENGLAND MARINE RSCH LAB / LIB, DUXBURY, MA
BELVOIR R&DC / COLONEL NEWMAN, FT BELVOIR, VA
CHEM CORP / DEARBORN CHEM DIV LIB, LAKE ZURICH, IL
CORNELL UNIV / LIB, ITHACA, NY
GLIDDEN CO / RSCH LIB, STRONGSVILLE, OH
KTA-TATOR, INC / PITTSBURG, PA
LAWRENCE LIVERMORE NATL LAB / PLANT ENGRG LIB (L-654), LIVERMORE, CA
LOS ANGELES COUNTY / PW DEPT (J. VICELJA), HARBOR CITY, CA
MAYTAG / DURANT, NEWTON, IA
MC CLELLAND ENGRS, INC / LIB, HOUSTON, TX
MOBIL R&D CORP / OFFSHORE ENGRG LIB, DALLAS, TX
NATL ACADEMY OF SCIENCES / BRB, (SMEALLIE), WASHINGTON, DC
NAVEODTECHCEN / TECH LIB, INDIAN HEAD, MD
NAVFACENGCOM / CODE 04A1D, ALEXANDRIA, VA
NAVFACENGCOM / CODE 04A3, ALEXANDRIA, VA
NAVFACENGCOM / CODE 04A3C, ALEXANDRIA, VA
NAVFACENGCOM / CODE 04B3, ALEXANDRIA, VA
NAVFACENGCOM / CODE 051A, ALEXANDRIA, VA
NAVFACENGCOM / CODE 1002B, ALEXANDRIA, VA
NAVFACENGCOM / CODE 163, ALEXANDRIA, VA
NAVFACENGCOM / CODE DS02, ALEXANDRIA, VA
NAVFACENGCOM CHESDIV / CODE 112.1, WASHINGTON, DC
NAVFACENGCOM CHESDIV / CODE 402 (FRANCIS), WASHINGTON, DC
NAVFACENGCOM CHESDIV / CODE 407, WASHINGTON, DC
NAVFACENGCOM CHESDIV / YACHNIS, WASHINGTON, DC
NAVFACENGCOM LANTDIV / CODE 403, NORFOLK, VA
NAVFACENGCOM NORTHDIV / CO, PHILADELPHIA, PA
NAVSHIPYD / CODE 244.13, LONG BEACH, CA
NAVSHIPYD / TECH LIB, PORTSMOUTH, NH
NAVSURFWARCEN COASTSYSTA / CODE 0222, PANAMA CITY, FL
NBS / BLDG MAT DIV, MATHEY, GAITHERSBURG, MD
NCCOSC / CODE 9642, SAN DIEGO, CA
NETPMSA / TECH LIB, PENSACOLA, FL
NEW ZEALAND CONCRETE RSCH ASSN / LIB, PORIRUA,
NIST / BLDG TECH, MCKNIGHT, GAITHERSBURG, MD

NOAA / LIB, ROCKVILLE, MD
NUSC DET / LIB, NEWPORT, RI
NY CITY COMMUNITY COLLEGE / LIB, BROOKLYN, NY
PENNSYLVANIA STATE UNIV / RSCH LAB, STATE COLLEGE, PA
SOUTHWEST RSCH INST / M. POLCYN, SAN ANTONIO, TX
SOUTHWEST RSCH INST / THACKER, SAN ANTONIO, TX
SUPSHIP / TECH LIB, NEWPORT, VA
TECHNOLOGY UTILIZATION / K WILLINGER, WASHINGTON, DC
UNIV OF DELAWARE / ENGRG COL (DEXTER), LEWES, DE
UNIV OF HAWAII / MANOA, LIB, HONOLULU, HI
UNIV OF TEXAS / CONSTRUCTION INDUSTRY INST, AUSTIN, TX
UNIV OF TEXAS / ECJ 4.8 (BREEN), AUSTIN, TX
UNIV OF TEXAS / ECJ 5.402 (TUCKER), AUSTIN, TX
UNIV OF WISCONSIN / GREAT LAKES STUDIES CEN, MILWAUKEE, WI
USAE / CEWES-IM-MI-R, VICKSBURG, MS
VALLEY FORGE CORPORATE CENTER / FRANKLIN RESEARCH CENTER, NORRISTOWN, PA
WESTINGHOUSE ELECTRIC CORP / LIB, PITTSBURG, PA
WOODWARD-CLYDE CONSULTANTS / WEST REG, LIB, OAKLAND, CA

DISTRIBUTION QUESTIONNAIRE

The Naval Civil Engineering Laboratory is revising its primary distribution lists.

SUBJECT CATEGORIES

1 **SHORE FACILITIES**
1A Construction methods and materials (including corrosion control, coatings)
1B Waterfront structures (maintenance/deterioration control)
1C Utilities (including power conditioning)
1D Explosives safety
1E Aviation Engineering Test Facilities
1F Fire prevention and control
1G Antenna technology
1H Structural analysis and design (including numerical and computer techniques)
1J Protective construction (including hardened shelters, shock and vibration studies)
1K Soil/rock mechanics
1L Airfields and pavements
1M Physical security
2 **ADVANCED BASE AND AMPHIBIOUS FACILITIES**
2A Base facilities (including shelters, power generation, water supplies)
2B Expedient roads/airfields/bridges
2C Over-the-beach operations (including breakwaters, wave forces)
2D POL storage, transfer, and distribution
2E Polar engineering
3 **ENERGY/POWER GENERATION**
3A Thermal conservation (thermal engineering of buildings, HVAC systems, energy loss measurement, power generation)
3B Controls and electrical conservation (electrical systems, energy monitoring and control systems)
3C Fuel flexibility (liquid fuels, coal utilization, energy from solid waste)
3D Alternate energy source (geothermal power, photovoltaic power systems, solar systems, wind systems, energy storage systems)
3E Site data and systems integration (energy resource data, integrating energy systems)
3F EMCS design
4 **ENVIRONMENTAL PROTECTION**
4A Solid waste management
4B Hazardous/toxic materials management
4C Waterwaste management and sanitary engineering
4D Oil pollution removal and recovery
4E Air pollution
4F Noise abatement
5 **OCEAN ENGINEERING**
5A Seafloor soils and foundations
5B Seafloor construction systems and operations (including diver and manipulator tools)
5C Undersea structures and materials
5D Anchors and moorings
5E Undersea power systems, electromechanical cables, and connectors
5F Pressure vessel facilities
5G Physical environment (including site surveying)
5H Ocean-based concrete structures
5J Hyperbaric chambers
5K Undersea cable dynamics

ARMY FEAP
BDG Shore Facilities
NRG Energy
ENV Environmental/Natural Responses
MGT Management
PRR Pavements/Railroads

TYPES OF DOCUMENTS

D = Techdata Sheets; **R** = Technical Reports and Technical Notes; **G** = NCEL Guides and Abstracts; **I** = Index to TDS; **U** = User Guides; ☐ None - remove my name

Old Address:

_____

_____

_____

_____

Telephone No.: _____

New Address:

_____

_____

_____

_____

Telephone No.: _____

INSTRUCTIONS

The Naval Civil Engineering Laboratory has revised its primary distribution lists. To help us verify our records and update our data base, please do the following:

- Add - circle number on list
- Remove my name from all your lists - check box on list.
- Change my address - line out incorrect line and write in correction **(DO NOT REMOVE LABEL).**
- Number of copies should be entered after the title of the subject categories you select.
- Are we sending you the correct type of document? If not, circle the type(s) of document(s) you want to receive listed on the back of this card.

Fold on line, staple, and drop in mail.

DEPARTMENT OF THE NAVY
Naval Civil Engineering Laboratory
560 Laboratory Drive
Port Hueneme CA 93043-4328

Official Business
Penalty for Private Use, $300

NO POSTAGE NECESSARY IF MAILED IN THE UNITED STATES

BUSINESS REPLY CARD
FIRST CLASS PERMIT NO. 12503 WASH D.C.

POSTAGE WILL BE PAID BY ADDRESSEE

COMMANDING OFFICER
CODE L34
560 LABORATORY DRIVE
NAVAL CIVIL ENGINEERING LABORATORY
PORT HUENEME CA 93043-4328

NCEL DOCUMENT EVALUATION

You are number one with us; how do we rate with you?

We at NCEL want to provide you our customer the best possible reports but we need your help. Therefore, I ask you to please take the time from your busy schedule to fill out this questionnaire. Your response will assist us in providing the best reports possible for our users. I wish to thank you in advance for your assistance. I assure you that the information you provide will help us to be more responsive to your future needs.

R. N. STORER, Ph.D, P.E.
Technical Director

DOCUMENT NO. _____ TITLE OF DOCUMENT: _____

_____

Date: _____ Respondent Organization : _____

Name: _____ Activity Code: _____
Phone: _____ Grade/Rank: _____

Category (*please check*):

Sponsor ____ User ____ Proponent ____ Other (*Specify*) _____

Please answer on your behalf only; not on your organization's. Please check (*use an X*) only the block that most closely describes your attitude or feeling toward that statement:

SA Strongly Agree A Agree O Neutral D Disagree SD Strongly Disagree

---

	SA	A	N	D	SD
1. The technical quality of the report is comparable to most of my other sources of technical information.	( )	( )	( )	( )	( )
2. The report will make significant improvements in the cost and or performance of my operation.	( )	( )	( )	( )	( )
3. The report acknowledges related work accomplished by others.	( )	( )	( )	( )	( )
4. The report is well formatted.	( )	( )	( )	( )	( )
5. The report is clearly written.	( )	( )	( )	( )	( )
6. The conclusions and recommendations are clear and directly supported by the contents of the report.	( )	( )	( )	( )	( )
7. The graphics, tables, and photographs are well done.	( )	( )	( )	( )	( )

Do you wish to continue getting NCEL reports? ☐ YES ☐ NO

Please add any comments (e.g., in what ways can we improve the quality of our reports?) on the back of this form.

Comments:

Fold on line, staple, and drop in mail.

DEPARTMENT OF THE NAVY
Naval Civil Engineering Laboratory
560 Laboratory Drive
Port Hueneme CA 93043-4328

Official Business
Penalty for Private Use, $300

NO POSTAGE NECESSARY IF MAILED IN THE UNITED STATES

BUSINESS REPLY CARD

FIRST CLASS PERMIT NO. 12503 WASH D.C.

POSTAGE WILL BE PAID BY ADDRESSEE

COMMANDING OFFICER
CODE L03
560 LABORATORY DRIVE
NAVAL CIVIL ENGINEERING LABORATORY
PORT HUENEME CA 93043-4328